Eclética Química Journal

Volume 43 • number 4 • year 2018

Synthesis, characterization and comparative thermal degradation study of Co(II), Ni(II) and Cu(II) complexes with Asparagine and Urea as mixed ligands

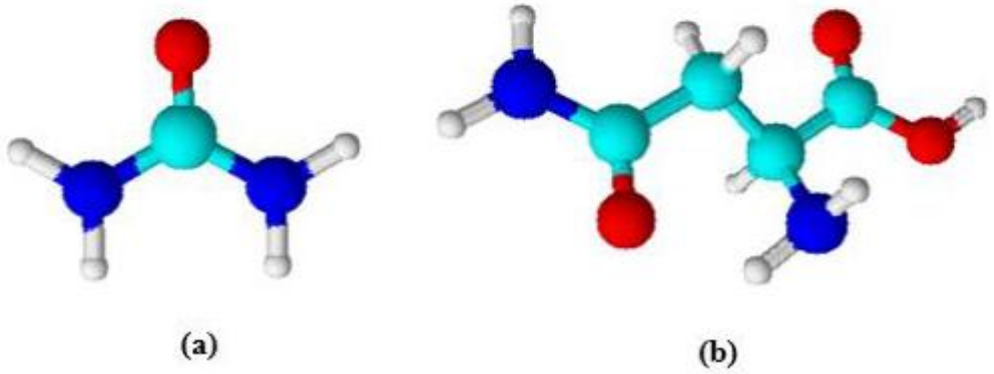

Figure 1. Structures of urea (a) and asparagine (b) molecules.

Ligands

Physicochemical and biological activity studies on complexes of some transition elements with mixed ligands of glycine and urea

Quality control

Simple, fast and inexpensive method for determination of ranitidine hydrochloride based on conductometric measurements

DNA breathing

Dark breather using symmetric morse, solvent and external potentials for DNA breathing

unesp
UNIVERSIDADE ESTADUAL PAULISTA
"JÚLIO DE MESQUITA FILHO"

Instituto de Química
UNESP
Araraquara
ISSN 1678-4618

UNIVERSIDADE ESTADUAL PAULISTA

Reitor

Sandro Roberto Valentini

Vice-reitor

Sergio Roberto Nobre

Pró-reitor de Planejamento Estratégico e Gestão

Leonardo Theodoro Büll

Pró-reitora de Graduação

Gladis Massini-Cagliari

Pró-reitor de Pós-Graduação

João Lima Sant'Anna Neto

Pró-reitora de Extensão Universitária

Cleopatra da Silva Planeta

Pró-reitor de Pesquisa

Carlos Frederico de Oliveira Graeff

INSTITUTO DE QUÍMICA

Diretor

Eduardo Maffud Cilli

Vice-Diretora

Dulce Helena Siqueira Silva

Eclética Química Journal

Editorial Team
iq.unesp.br/ecletica

| Vol. 43 | n. 4 | 2018 |

Editorial Team

Editors

Prof. Assis Vicente Benedetti, Institute of Chemistry Unesp Araraquara, Brazil (Editor-in-Chief)
Prof. Arnaldo Alves Cardoso, Institute of Chemistry Unesp Araraquara, Brazil
Prof. Antonio Eduardo Mauro, Institute of Chemistry Unesp Araraquara, Brazil
Prof. Horacio Heinzen, Faculty of Chemistry UdelaR, Montevideo, Uruguay
Prof. Maysa Furlan, Institute of Chemistry Unesp Araraquara, Brazil
Prof. Maria Célia Bertolini, Institute of Chemistry Unesp Araraquara, Brazil
Prof. Paulo Clairmont Feitosa de Lima Gomes, Institute of Chemistry, Unesp Araraquara, Brazil

Editorial Board

Prof. Jairton Dupont, Instituto de Química, Universidade Federal do Rio Grande do Sul, UFRGS, RS, Brazil
Prof. Enric Brillas, Facultat de Química, Universitat de Barcelona, Spain
Prof. Verónica Cortés de Zea Bermudez, Escola de Ciências da Vida e do Ambiente,Universidade de Trás-os-Montes e Alto Douro, Vila Real, Portugal
Prof. Lauro Kubota, Instituto de Química, Universidade Estadual de Campinas, Unicamp, SP, Brazil
Prof. Ivano Gerardt Rolf Gutz, Instituto de Química, Universidade de São Paulo, USP, SP, Brazil
Prof. Massuo Jorge Kato, Instituto de Química, Universidade de São Paulo, USP, SP, Brazil
Prof. Francisco de Assis Leone, Faculdade de Filosofia, Ciências e Letras, Universidade de São Paulo, Ribeirão Preto, USP-RP, SP, Brazil
Prof. Roberto Santana da Silva, Faculdade de Ciências Farmacêuticas, Universidade de São Paulo, Ribeirão Preto, USP-RP, SP, Brazil
Prof. José Antônio Maia Rodrigues, Faculdade de Ciências, Universidade do Porto, Portugal
Prof. Bayardo Baptista Torres, Instituto de Química, Universidade de São Paulo, USP, SP, Brazil

Technical Staff

Gustavo Marcelino de Souza
Lucas Henrique de Carvalho Machado

Eclética Química Journal

Editorial
iq.unesp.br/ecletica

| Vol. 43 | n. 4 | 2018 |

Editorial

In the twilight of this year, the readers of Eclética Química Journal will find in this last issue interesting articles dealing with the synthesis and extensive physicochemical characterization of cobalt, nickel and copper complexes containing mixed ligands such as urea and glycine or urea and asparagine for which an octahedral structure was proposed. Antibacterial assays with *Bacillus* spp., *Escherichia coli*, *Pseudomonas aeruginosa* and *Staphylococcus aureus* were performed for the metallic complexes containing urea and glycine, but only the nickel derivative showed some activity against *Escherichia coli*. In the sequence, the developing of a fast, simple and inexpensive alternative method for determining ranitidine in generic formulations without any sample pretreatment was described. It was based on conductometric titration of ranitidine hydrochloride by precipitation of AgCl using a solution of $AgNO_3$ as titrant. In another investigation, the dynamics and the quantum thermodynamics of DNA in Symmetric-Peyrard-Bishop-Dauxois model (S-PBD) with solvent and external potentials were analyzed and the transient conformational fluctuations using dark breather and the ground state wave function of the associate Schrodinger differential equation was described.

Assis Vicente Benedetti
Editor-in-Chief of EQJ

Eclética Química Journal

Author guidelines
iq.unesp.br/ecletica

| Vol. 43 | n. 4 | 2018 |

Instructions for Authors

Preparation of manuscripts

• **Only manuscripts in English will be accepted.** British or American usage is acceptable, but they should not be mixed.

• **The corresponding author should submit the manuscript online**: http://revista.iq.unesp.br/ojs/index.php/ecletica/author

• **Manuscripts must be sent in editable files as** *.doc, *.docx or *.odt. The text must be typed using font style Times New Roman and size 11. Space between lines should be 1.5 mm and paper size A4.

• **The manuscript should be organized in sections as follows:** Introduction, Experimental, Results and Discussion, Conclusions, and References. Sections titles must be written in bold and numbered sequentially; only the first letter should be in uppercase letter. Subsections should be written in normal and italic lowercase letters. For example: **1. Introduction**; *1.1 History;* **2. Experimental**; *2.1 Surface characterization; 2.1.1 Morphological analysis.*

• **The cover letter should include**: the authors' full names, e-mail addresses, ORCID code and affiliations, and remarks about the novelty and relevance of the work. The cover letter should also contain a declaration of the corresponding author, on behalf of the other authors, that the article being submitted is original and its content has not been published previously and is not under consideration for publication elsewhere, that no conflict of interest exists and if accepted, the article will not be published elsewhere in the same form, in any language, without the written consent of the publisher. Finally, the cover letter should also contain the suggestion of 3 (three) suitable reviewers (please, provide full name, affiliation, and e-mail).

• **The first page of the manuscript** should contain the title, abstract and keywords. ***Please, do not give authors names and affiliation, and acknowledgements since a double-blind reviewer system is used. Acknowledgements should be added to the proof only*.**

• **All contributions should include** an Abstract (200 words maximum), three to five Keywords and a Graphical Abstract (8 cm wide and 4 cm high) with an explicative text (2 lines maximum).

• **References should be numbered** sequentially in superscript throughout the text and compiled in brackets at the end of the manuscript as follows:

***Journal*:**

[1] Adorno, A. T. V., Benedetti, A. V., Silva, R. A. G. da, Blanco, M., Influence of the Al content on the phase transformations in Cu-Al-Ag Alloys, Eclet. Quim. 28 (1) (2003) 33-38. https://doi.org/10.1590/S0100-46702003000100004.

***Book*:**

[2] Wendlant, W. W., Thermal Analysis, Wiley-Interscience, New York, 3rd ed., 1986, ch1.

***Chapter in a book*:**

[3] Ferreira, A. A. P., Uliana, C. V., Souza Castilho, M. de, Canaverolo Pesquero, N., Foguel, N. V., Pilon dos Santos, G., Fugivara, C. S., Benedetti, A. V., Yamanaka, H., Amperometric Biosensor for Diagnosis of Disease, In: State of the Art in Biosensors - Environmental and Medical Applications, Rinken, T., ed., InTech: Rijeka, Croatia, 2013, Ch. 12.

***Material in process of publication*:**

[4] Valente Jr., M. A. G., Teixeira, D. A., Lima Azevedo, D., Feliciano, G. T., Benedetti, A. V., Fugivara, C. S., Caprylate Salts Based on Amines as Volatile Corrosion Inhibitors for Metallic Zinc: Theoretical and Experimental Studies, Frontiers in Chemistry. https://doi.org/10.3389/fchem.2017.00032.

• Figures, Schemes, and Tables should be numbered sequentially and presented at the end of the manuscript.

• Nomenclature, abbreviations, and symbols should follow IUPAC recommendations.

• Figures, schemes, and photos already published by the same or different authors in other publications may be reproduced in manuscripts of **Eclet. Quim. J.** only with permission from the editor house that holds the copyright.

• Graphical Abstract (GA) should be a high-resolution figure (900 dpi) summarizing the manuscript in an interesting way to catch the attention of the readers and accompanied by a short explicative text (2 lines maximum). GA must be submitted as *.jpg, *.jpeg or *.tif.

• **Communications** should cover relevant scientific results and are limited to 1,500 words or three pages of the Journal, not including the title, authors' names, figures, tables and references. However, Communications suggesting fragmentation of complete contributions are strongly discouraged by Editors.

• **Review articles** should be original and present state-of-the-art overviews in a coherent and concise form covering the most relevant aspects of the topic that is being revised and indicate the likely future directions of the field. Therefore, before beginning the preparation of a Review manuscript, send a letter (1page maximum) to the Editor with the subject of interest and the main topics that would be covered in Review manuscript. The Editor will communicate his decision in two weeks. Receiving this type of manuscript does not imply acceptance to be published in **Eclet. Quím. J.** It will be peer-reviewed.

• **Short reviews** should present an overview of the state-of-the-art in a specific topic within the scope of the Journal and limited to 5,000 words. Consider a table or image as corresponding to 100 words. Before beginning the preparation of a Short Review manuscript, send a letter (1page maximum) to the Editor with the subject of interest and the main topics that would be covered in the Short Review manuscript.

• **Technical Notes**: descriptions of methods, techniques, equipment or accessories developed in the authors' laboratory, as long as they present chemical content of interest. They should follow the usual form of presentation, according to the peculiarities of each work. They should have a maximum of 15 pages, including figures, tables, diagrams, etc.

• **Articles in Education in Chemistry and chemistry-correlated areas**: research manuscript related to undergraduate teaching in Chemistry and innovative experiences in undergraduate and

graduate education. They should have a maximum of 15 pages, including figures, tables, diagrams, and other elements.

• **Special issues** with complete articles dedicated to Symposia and Congresses can be published by **Eclet. Quim. J.** under the condition that a previous agreement with Editors is established. All the guides of the journal must be followed by the authors.

• **Eclet. Quim. J.** Ethical Guides and Publication Copyright:

Before beginning the submission process, please be sure that all ethical aspects mentioned below were followed. Violation of these ethical aspects may prevent authors from submitting and/or publishing articles in **Eclet. Quim. J.**

- The corresponding author is responsible for listing as authors only researchers who have really taken part in the work, and for informing them about the entire manuscript content and for obtaining their permission for submitting and publishing.

- Authors are responsible for carefully searching for all the scientific work relevant to their reasoning irrespective of whether they agree or not with the presented information.

- Authors are responsible for correctly citing and crediting all data used from works of researchers other than the ones who are authors of the manuscript that is being submitted to **Eclet. Quim. J.**

- Citations of Master's Degree Dissertations and PhD Theses are not accepted; instead, the publications resulting from them must be cited.

- Explicit permission of a non-author who has collaborated with personal communication or discussion to the manuscript being submitted to **Eclet. Quím. J.** must be obtained before being cited.

- Simultaneous submission of the same manuscript to more than one journal is considered an ethical deviation and is conflicted to the declaration has been done below by the authors.

- Plagiarism, self-plagiarism, and the suggestion of novelty when the material was already published are unaccepted by **Eclet. Quim. J.**

- The word-for-word reproduction of data or sentences as long as placed between quotation marks and correctly cited is not considered ethical deviation when indispensable for the discussion of a specific set of data or a hypothesis.

- Before reviewing a manuscript, the *turnitin* anti-plagiarism software will be used to detect any ethical deviation.

- The corresponding author transfers the copyright of the submitted manuscript and all its versions to **Eclet. Quim. J.**, after having the consent of all authors, which ceases if the manuscript is rejected or withdrawn during the review process.

- Before submitting manuscripts involving human beings, materials from human or animals, the authors need to confirm that the procedures established, respectively, by the institutional committee on human experimentation and Helsinki's declaration, and the recommendations of the animal care institutional committee were followed. Editors may request complementary information on ethical aspects.

- When a published manuscript in EQJ is also published in other Journal, it will be immediately withdrawn from EQJ and the authors informed of the Editor decision.

• Manuscript Submissions

For the first evaluation: the manuscripts should be submitted in three files: the cover letter as mentioned above, the graphical abstract and the entire manuscript.

The entire manuscript should be submitted as *.doc, *.docx or *.odt files.

The Graphical Abstract (GA) 900 dpi resolution is mandatory for this Journal and should be submitted as *.jpg, *.jpeg or *.tif files as supplementary file.

The cover letter should contain the title of the manuscript, the authors' names and affiliations, and the relevant aspects of the manuscript (no more than 5 lines), and the suggestion of 3 (three) names of experts in the subject: complete name, affiliation, and e-mail).

• Reviewing

The time elapsed between the submission and the first response of the reviewers is around 3 months. The average time elapsed between submission and publication is 7 months.

• **Resubmission** (manuscripts "rejected in the present form" or subjected to "revision"): **A LETTER WITH THE RESPONSES TO THE COMMENTS/CRITICISM AND SUGGESTIONS OF REVIEWERS/EDITORS SHOULD ACCOMPANY THE REVISED MANUSCRIPT. ALL MODIFICATIONS MADE TO THE ORIGINAL MANUSCRIPT MUST BE HIGHLIGHTED.**

• Editor's requirements

Authors who have a manuscript accepted in **Eclética Química Journal** may be invited to act as reviewers.

Only the authors are responsible for the correctness of all information, data and content of the manuscript submitted to **Eclética Química Journal**. Thus, the Editors and the Editorial Board cannot accept responsibility for the correctness of the material published in **Eclética Química Journal**.

• Proofs

After accepting the manuscript, **Eclet. Quim. J.** technical assistants will contact you regarding your manuscript page proofs to correct printing errors only, i.e., other corrections or content improvement are not permitted. The proofs shall be returned in 3 working days (72 h) via e-mail.

• Authors Declaration

The corresponding author declares, on behalf of the other authors, that the article being submitted is original and has been written by the stated authors who are all aware of its content and approve its submission. Declaration should also state that the article has not been published previously and is not under consideration for publication elsewhere, that no conflict of interest exists and if accepted, the article will not be published elsewhere in the same form, in any language, without the written consent of the publisher.

• Appeal

Authors may only appeal once about the decision regarding a manuscript. To appeal against the Editorial decision on your manuscript, the corresponding author can send a rebuttal letter to the editor, including a detailed response to any comments made by the reviewers/editor. The editor will consider the rebuttal letter, and if dimmed appropriate, the manuscript will be sent to a new reviewer. The Editor decision is final.

• Contact

Gustavo Marcelino de Souza (ecletica@journal.iq.unesp.br)

Submission Preparation Checklist

As part of the submission process, authors are required to check off their submission's compliance with all of the following items, and submissions may be returned to authors that do not adhere to these guidelines.

In **Step 1**, select the appropriate section for this submission.

Be sure that Authors' names, affiliations and aknowledgements were removed from the manuscript. The manuscript must be in *.doc, *.docx or *.odt format before uploading in **Step 2**.

In **Step 3**, add the full name of each author including the ORCID IDs in its full URL ONLY WITH HTTP, NOT HTTPS (eg. http://orcid.org/0000-0002-1825-0097).

Add the authors in the same order as they appear in the manuscript in **step 3**.

Be sure to have the COVER LETTER and GRAPHICAL ABSTRACT (according to the Author Guildelines) to upload them in **Step 4**.

Check if you've followed all the previous steps before continuing the submission of your manuscript.

Copyright Notice

The corresponding author transfers the copyright of the submitted manuscript and all its versions to **Eclet. Quim. J.**, after having the consent of all authors, which ceases if the manuscript is rejected or withdrawn during the review process.

Self-archive to institutional, thematic repositories or personal web page is permitted just after publication.

The articles published by **Eclética Química Journal** are licensed under the Creative Commons Attribution 4.0 International License.

Eclética Química Journal

Summary
iq.unesp.br/ecletica

| Vol. 43 | n. 4 | 2018 |

SUMMARY

EDITORIAL BOARD.....3
EDITORIAL.....4
INSTRUCTIONS FOR AUTHORS.....5

ORIGINAL ARTICLES
Synthesis, characterization and comparative thermal degradation study of Co(II), Ni(II) and Cu(II) complexes with Asparagine and Urea as mixed ligands.....11
Yasmin Mosa'd Jamil, *Maher Ali Al-Maqtari*, *Fathi Mohammed Al-Azab*, *Mohammed Kassem Al-Qadasy*, *Amani A. Al-Gaadbi*

Physicochemical and biological activity studies on complexes of some transition elements with mixed ligands of glycine and urea.....25
Maher Ali Al-Maqtari, *Mohammed Kassem Al-Qadasy*, *Yasmin Mosa'd Jamil, Fathi Mohammed Al-Azab, Amani A. Al-Gaadbi*

Simple, fast and inexpensive method for determination of ranitidine hydrochloride based on conductometric measurements.....36
Eduardo Henrique Bindewald, João Carlos da Rosa-Sobrinho, Márcio Fernando Bergamini, Luiz Humberto Marcolino-Júnior

Dark breather using symmetric morse, solvent and external potentials for DNA breathing.....43
Hernán Oscar Cortez Gutierrez, Milton Milciades Cortez Gutierrez, Girady Iara Cortez Fuentes Rivera, Liv Jois Cortez Fuentes Rivera, Deolinda Fuentes Rivera Vallejo

Eclética Química Journal

Original article
iq.unesp.br/ecletica

| Vol. 43 | n. 4 | 2018 |

Synthesis, characterization and comparative thermal degradation study of Co(II), Ni(II) and Cu(II) complexes with Asparagine and Urea as mixed ligands

Yasmin Mosa'd Jamil[1+], Maher Ali Al-Maqtari[1], Fathi Mohammed Al-Azab[1], Mohammed Kassem Al-Qadasy[1], Amani A. Al-Gaadbi[1]

[1] Sana'a University, Faculty of Science, Chemistry Department, Sana'a, Yemen

[+] Corresponding author: Yasmin Mosa'd Jamil, e-mail address: yasminjml@yahoo.com

ARTICLE INFO

Article history:
Received: March 12, 2018
Accepted: May 14, 2018
Published: December 5, 2018

Keywords:
1. urea
2. asparagine
3. transition elements complexes
4. thermal analysis

ABSTRACT: New Co(II), Ni(II) and Cu(II) complexes with urea and asparagine as ligands have been synthesized in ($M:L_1:L_2$) molar ratio (where M= Co(II), Ni(II) and Cu(II), L_1 = urea, and L_2 = asparagine) then identified by micro analyses, molar conductance measurements, IR, ^{1}HNMR, Mass, UV-VIS spectroscopies and magnetic susceptibility measurements. Thermal degradation studies were carried out by thermal analysis. These complexes have the general formula $[M(L_1)(L_2)(H_2O)_n]Cl$. The molar conductance values in DMSO solvent show the electrolytic nature of these complexes, indicating the outer-sphere coordination of the chloride anions with metal ions. The three complexes have an octahedral structure with urea molecule showing two modes of coordination. Thermal analysis study shows the rapid decomposition reaction for Ni complex and the highest thermal stability for Cu complex. The kinetic parameters were determined from the thermal decomposition data using the Coats-Redfern method. Thermodynamic parameters were calculated using standard relations.

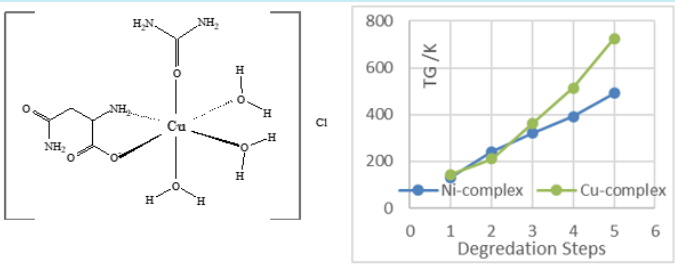

New complexes of urea and asparagine coordinated to M (Co^{2+}, Ni^{2+} and Cu^{2+}) were prepared and an octahedral structure was proposed. Cu complex presented higher thermal stability.

1. Introduction

Recently, there has been renewed attention in the preparation and studies of mixed ligand transition metal complexes[1, 2] due to their new useful properties such as magnetic exchange, photoluminescence, nonlinear optical property, electrical conductivity and antimicrobial activity[3-5].

Mixed ligand complexes containing amino acid as co-ligand are potential biomimetic models for metal-protein interaction[6]. Research has shown significant progress in utilization of transition metal complexes as drugs to treat a lot of human diseases like carcinomas, infection control, anti-inflammatory, diabetes and neurological disorders[7].

Urea, carbamide or carbonyldiamide $CO(NH_2)_2$ (Figure 1a), which has a remarkable role in many biological processes in decomposition of proteins and amino acid catabolism, was discovered in 1828 by Wöhler when evaporating a solution containing a mixture of potassium isocyanate and ammonium sulphate[8].

The mode of urea bonding with metal ions seems to be dependent upon the type and nature of the metal, lead(II) coordinates to the nitrogen atom, whereas iron(III), zinc(II) and copper(II)

coordinate to the oxygen of urea[9]. Also, there are different types of coordination of urea in its complexes with rare-earth iodides and perchlorates[10].

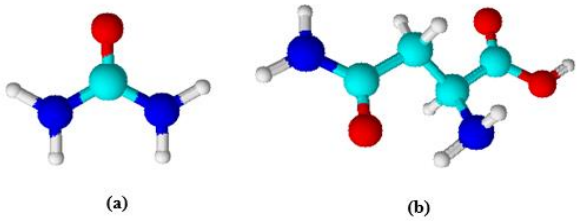

Figure 1. Structures of urea (a) and asparagine (b) molecules.

The amino acids are the main building units of all various forms of life and were earlier discovered as ingredient of natural products even before they were recognized as components of proteins[11]. The amino acid L-asparagine or 2-amino-3-carbamoylpropanoic acid (Fig. 1b) is a structural analog of L-aspartic acid. It was the first amino acid to be isolated from plants 200 years ago and because it has an N:C ratio of 2:4, this makes it an efficient molecule for the storage and transport of nitrogen in living organisms[12]. There are some similar thermal studies of various types of mixed ligands with transition metals[1, 2, 13-15], however, no previous studies on the synthesis, characterization and thermal studies of the mixed ligand complexes of urea and asparagine acid have been reported. Hence, the present work reports the preparation, characterization and thermal study of new mixed ligand complexes of urea and asparagine with Co(II), Ni(II) and Cu(II) ions.

2. Materials and methods

2.1 Chemicals

All chemicals such as solvents, metal(II) chlorides (i.e. $CoCl_2.6H_2O$, $NiCl_2.6H_2O$ and $CoCl_2.2H_2O$) were commercially available from BDH and were used without further purification.

2.2 Instrumentation

The melting points of the metal complexes were measured in glass capillary tubes with a Stuart Scientific Electrothermal melting point apparatus. TLC was carried out on silica gel GF_{254} plates (mn-kieselgel G., 0.2 mm thickness) with a 3:1 v/v ethyl acetate / petroleum ether solution as eluent mobile at room temperature. The plates were scanned under ultraviolet light lamp of 254 nm. The CHN elemental analysis of the complexes was carried out by Vario ELFab. Chloride was determined volumetrically by silver nitrate. The amount of H_2O was determined gravimetrically using weight loss method. Perkin-Elmer 2380 flame atomic absorption spectrophotometer was used for the determination of metal content. Jenway conductivity meter model 4510 was used for measuring the molar conductance of the freshly prepared metal complexes solutions (10^{-3} mol L^{-1} in DMSO) at room temperature. IR spectra of the metal complexes were measured in the range 200-4000 cm^{-1} with a FT/IR–140 (Jasco, Japan). Varian FT-300 MHz spectrometer was used for recording ^{1}HNMR spectra in d_6DMSO solvent and TMS as internal standard. Mass spectra were recorded in a Jeol JMS600 spectrometer. The electronic spectra of the complexes were measured in the range 400–800 nm, using UV–VIS spectrophotometer Specord 200, Analytilk Jena (Germany). The magnetic susceptibility of the solid complexes was measured at room temperature using Gouy's method by a balance from Johnson Metthey and Sherwood model. The Differential Thermal Analysis (DTA) and Thermogravimetric Analysis (TGA) experiments were performed under nitrogen atmosphere using a platinum sample pan at a flow rate of 30 mL min^{-1} and a 10 °C min^{-1} heating rate for the temperature range 25–800 °C in Shimadzu DTA-50 and Shimadzu TGA-50H thermal analyzers, respectively, at Micro Analytical Center, Cairo University, Egypt.

2.3 Synthesis of mixed ligand complexes

Generally, the solid complexes were prepared by adding dropwise an ethanolic solution of hydrated metal(II) chlorides (0.01 mol) to an ethanolic solution of urea (0.01 mol) with stirring. The mixture was refluxed for 12 h with persistent stirring. A hot solution of 0.01 mol asparagine in 1:1 ethanol / water mixture ratio with drops of 1 mol L^{-1} NaOH was used to adjust the pH at 7-7.5 and to deprotonate NH_3^+ in the asparagine to NH_2. The mixture was refluxed for 2 h until the formation of colored precipitate occurred. All the solutions were in 1:1:1 molar ratio. The end products were filtered off and washed with distilled water to remove NaCl, followed by absolute ethanol until the solution became clear, and after

Eclética Química Journal, vol. 43, n. 4, 2018, 11-24
ISSN: 1678-4618
DOI: 10.26850/1678-4618eqj.v43.4.2018.p11-24

that the product was washed with DMF and left to dry[16]. The yield was 56%, 52% and 42% for Co, Ni and Cu-complexes, respectively.

3. Results and discussion

Complexes of Co(II), Ni(II) and Cu(II) with urea and asparagine are studied. Some physical properties, molar conductivity and analytical data are summarized in Tables 1 and 2. The elemental analysis proves that the complexes of Co(II), Ni(II) and Cu(II) with urea (ur) and asparagine (A_{asn}) ligands are of 1:1:1 (metal:ur:asn) molar ratio. The molar conductivity values indicate that the chloride anions are in the outer-sphere of these complexes.

Table 1. Some properties of the complexes.

Complex proposed formula	Color	M.p / °C	TLC		Molar conductivity Λ_m/S cm^2 mol^{-1}
			No. of spots	R_f	
$[Co(ur)(asn)(H_2O)_2]Cl$ $[Co(C_5H_{15}N_4O_6)]Cl$	dark violet	203±1	One	0.18	133
$[Ni(ur)(asn)(H_2O)_2]Cl$ $[Ni(C_5H_{15}N_4O_6)]Cl$	bluish green	185±1	One	0.24	128
$[Cu(ur)(asn)(H_2O)_3]Cl$ $[Cu(C_5H_{17}N_4O_7)]Cl$	light violet	337±1	One	0.32	140

Table 2. The elemental analysis of the complexes.

Complex proposed formula	Molecular weight		Elemental analysis									
			%C		%H		%N		%M		%Cl	
	calc.	found	calc.	found	calc.	found	calc.	found	calc.	found	calc.	found
$[Co(ur)(asn)(H_2O)_2]Cl$ $[Co(C_5H_{15}N_4O_6)]Cl$	321.58	321.61	18.67	18.67	4.70	4.70	17.42	17.42	18.33	18.32	11.03	11.04
$[Ni(ur)(asn)(H_2O)_2]Cl$ $[Ni(C_5H_{15}N_4O_6)]Cl$	321.34	321.36	18.68	18.69	4.70	4.71	17.44	17.44	18.27	18.26	11.03	11.05
$[Cu(ur)(asn)(H_2O)_3]Cl$ $[Cu(C_5H_{17}N_4O_7)]Cl$	344.21	344.23	17.44	17.45	4.98	4.89	16.28	16.28	18.46	18.46	10.29	10.31

3.1 IR Spectra of urea-asparagine complexes

In these complexes, urea acts in two ways: as a monodentate ligand through oxygen of C=O, or as a bidentate through nitrogen of two NH_2 groups, while asparagine acts as an anion bidentate molecule, through COO^- group and NH_2 group. The assignment of the distinctive bands is summarized in Table 3 and the IR spectra of complexes are shown in Figures 2 to 4.

The IR spectra of the complexes show additional broad bands in the range 3386-3430 cm^{-1} due to the υ(OH) stretching of water molecule. Coordinated water is also identified by the appearance of ρ_r (rocking) and ρ_w (wagging) approximately at 875 cm^{-1} and 521 cm^{-1}, respectively. These results agree with the elemental analysis and thermogravimetric studies[17]. The υ(NH_2) stretching vibrations of free urea at υ_s3353 cm^{-1} and υ_{as}3466 cm^{-1} were shifted to lower wave numbers in the spectra of the complexes of Co(II) and Ni(II). This fact shows that the υ(NH_2) group must be involved in coordination while υ(CO) shifted to higher frequency[18].

Eclética Química Journal, vol. 43, n. 4, 2018, 11-24
ISSN: 1678-4618
DOI: 10.26850/1678-4618eqj.v43.4.2018.p11-24

Table 3. Main IR bands (cm^{-1}) of the urea-asparagine complexes.

Urea	Asparagine	[Co(ur)(asn)(H_2O)$_2$]Cl	[Ni(ur)(asn)(H_2O)$_2$]Cl	[Cu(ur)(asn)(H_2O)$_3$]Cl	Assignment
-	3110m	-	-	-	$\upsilon(NH_3^+)$
3353m	3182m	ur-3320w asn-3185w,br asn-3227br	ur-3250 asn-3179br asn-3235br	ur-3298 m asn-3189br asn-3265 m	$\upsilon_s(NH_2)$
3466 m	3182m	ur-3420br asn-3185w,br asn-3320w,br	ur-3430br asn-3179br asn-3235br	ur-3337m asn-3189br asn- 3386m	$\upsilon_{as}(NH_2)$ H_2O, $\upsilon(OH)$
1618br	1644m	1637w	1637w	1629m	$\delta(NH)$
-	1428s	1412 s	1420w	1423w	$\upsilon_s(COO^-)$
-		1509 w	1509 w	1509w	$\upsilon_{as}(COO^-)$
1695w	1745w 1681m	ur-1719w asn-1773w asn-1662m	ur-1725 s asn-1773w asn-1655m	ur-1629m asn-1773w asn- 1665m	$\upsilon(CO)$
1468br	υ(C-N)1074s υ(O=C-N)1399m	ur-1446w asn-1081m asn-1409w,br	ur-1459m asn-1040 m asn-1410 w	ur-1490w asn-1039w asn1413m-	$\upsilon(C-N)$
-	2874w	2873 w	2858 m	2857w	$\upsilon(CH_2)$
-	1428s	1445w	1420w	1439w	$\delta(CH_2)$
-		472 w	476w	454m	$\upsilon(M-O)$
-		422w	421w	413m	$\upsilon(M-N)$

s = strong, m = medium, br = broad, w = weak, w,br = weak and broad

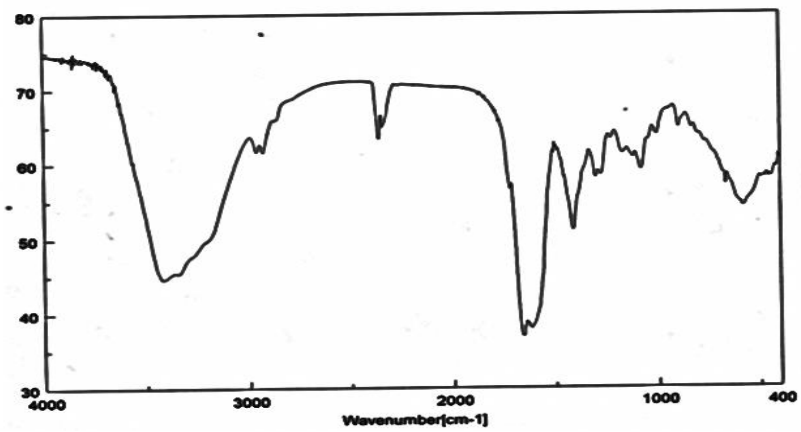

Figure 2. IR spectrum of [Co(ur)(asn)(H_2O)$_2$]Cl.

Eclética Química Journal, vol. 43, n. 4, 2018, 11-24
ISSN: 1678-4618
DOI: 10.26850/1678-4618eqj.v43.4.2018.p11-24

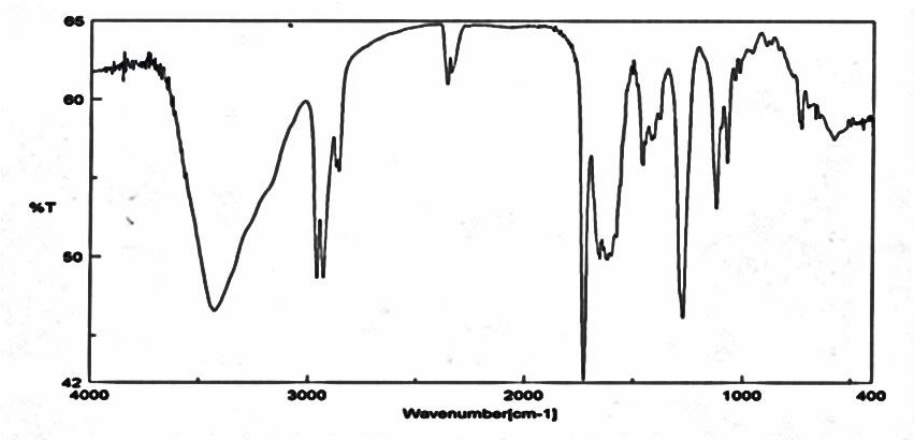

Figure 3. IR spectrum of $[Ni(ur)(asn)(H_2O)_2]Cl$.

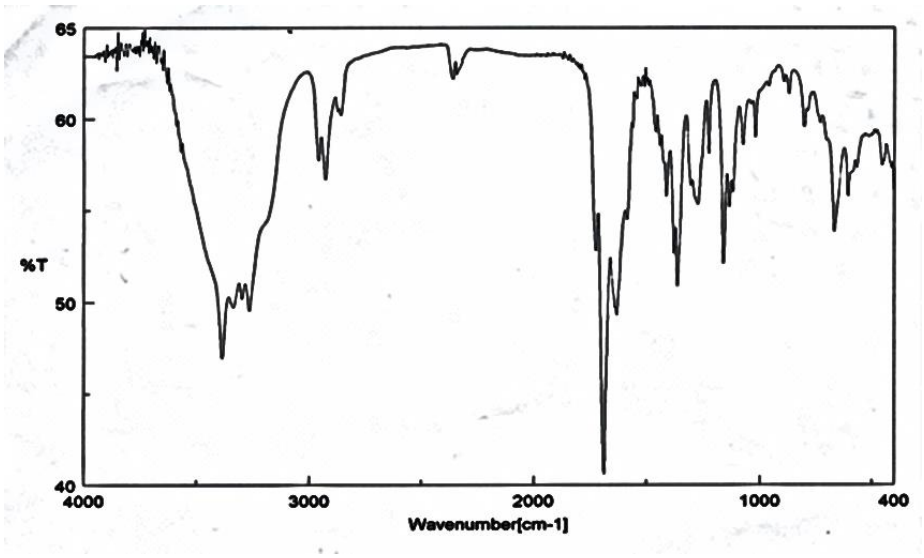

Figure 4. IR spectrum of $[Cu(ur)(asn)(H_2O)_3]Cl$.

The IR spectrum of the Cu(II)-complex showed a new band at 1629 cm^{-1} assigned to $\upsilon(C=O-Cu(II))$ with slight change in $\upsilon(NH_2)$ vibration[19]. In comparison with asparagine, $\upsilon_s(COO^-)$ and $\upsilon_{as}(COO^-)$ shift to lower wave numbers, confirming the monodentate nature of the coordinated carboxylate group[20].

The $\upsilon(NH_3^+)$ band at 3110 cm^{-1}, which is specific for the zwitterion in asparagine, vanished in the spectra of the complexes after the deprotonation of NH_3^+ to NH_2. Therefore, the higher wave numbers shift of the bands assigned to $\upsilon_{as}(NH_2)$ and $\upsilon_s(NH_2)$ indicates that the NH_2 group is imminently involved in the coordination[20].

IR of the prepared complexes showed weak bands in the range of 476-454 cm^{-1} and 422-413 cm^{-1}, attributed to $\upsilon(M-O)$ and $\upsilon(M-N)$, respectively[21]. Other bands are listed in Table 3.

3.2 ^{1}HNMR spectra of urea-asparagine complexes

^{1}HNMR spectra of $[Co(ur)(asn)(H_2O)_2]Cl$, $[Ni(ur)(asn)(H_2O)_2]Cl$ and $[Cu(ur)(asn)(H_2O)_3]Cl$ complexes show various signals which were summarized in Table 4. Urea shows a new signal at 5 and 5.1 ppm in Co(II) and Ni(II) complexes, respectively, for the amide groups coordinated to the metal atom without proton displacement[22], while in Cu(II) complex only carbonyl group is coordinated to metal[22]. The signals at 3.2, 3.1 and 2.85 ppm are assigned to CH group, whereas signals at 2.9, 2.45 and 2.5 ppm of CH_2 group are observed for Co(II), Ni(II) and Cu(II) complexes, respectively. The appearance of a new signal around 2.6-2.7 ppm is attributed to NH_2 group of asparagine and the amide group shows signals in the range 6.3-6.7 ppm[23]. The coordinated H_2O shows a new signal around 3.5-3.7 ppm[24].

Eclética Química Journal, vol. 43, n. 4, 2018, 11-24
ISSN: 1678-4618
DOI: 10.26850/1678-4618eqj.v43.4.2018.p11-24

Table 4. ^{1}HNMR chemical shift of free urea and asparagine ligands and their complexes.

System	$(CH)_\alpha$	$(CH)_\beta$	NH_3^+	$NH_{2(asn)}$	$NH_{2(ur)}$	H_2O
Urea	-	-	-	-	6-7.5	-
Asparagine	4.6	2.6	7-8	6.9-7.6	-	-
$[Co(ur)(asn)(H_2O)_2]Cl$	3.2	2.9	-	6.6, 2.7	$5_{(bonding)}$	3.7
$[Ni(ur)(asn)(H_2O)_2]Cl$	3.1	2.45	-	6.3, 2.7	$5.1_{(bonding)}$	3.55
$[Cu(ur)(asn)(H_2O)_3]Cl$	2.85	2.5	-	6.7. 2.6	$6.4_{(nonbonding)}$	3.5

3.3 Mass spectra of urea – asparagine complexes

The mass spectra of Co(II), Ni(II) and Cu(II) complexes with urea and asparagine ligands exhibited the molecular ion peaks at m/z (calc. 321.58, found 321.61; calc. 321.34, found 321.36 and calc. 344.21, found 344.23), respectively.

The molecular ion of $[Co(ur)(asn)(H_2O)_2]Cl$ complex loses NH_4Cl and $H_2NCH_2COO^-$ leaving ions at m/z 268.13 and 247.07, respectively; then loses NH_2 and H_2O fragments, giving an ion at m/z 212.08. The spectrum of $[Ni(ur)(asn)(H_2O)_2]Cl$ complex shows a peak at m/z 267.89, indicating the loss of H_2O and ½Cl_2. The molecule of $[Cu(ur)(asn)(H_2O)_3]Cl$ loses H_2O + NH_2 and ½Cl_2 + H_2O, leaving ions at m/z 310.07 and 290.76, respectively. The ion at m/z 310.07 loses CO_2, leaving an ion at m/z 266.09, which further loses ½N_2 to leave an ion at m/z 252.01. Afterwards, this last ion gives a new peak at m/z 234, indicating loss of H_2O and the remaining fragment loses another CO, leaving an ion at m/z 206.05.

3.4 Magnetic and electronic spectral studies

The electronic spectra of the Co(II), Ni(II) and Cu(II) complexes as well as their magnetic moment data have provided good evidence for the structures of these complexes as shown in Table 5. For $[Co(ur)(asn)(H_2O)_2]Cl$, hexa-coordination is suggested as in Figure 5a, based on the appearance of bands at 18248 cm^{-1} and at 14534 cm^{-1} (Figure 6), which were attributed to the $^4T_{1g}\rightarrow{}^4T_{1g}(P)$ (υ_3) and $^4T_{1g}\rightarrow{}^4A_{2g}$ (υ_2) transitions, respectively[25]. The third band, υ_1, could not be observed due to the limited range of the instrument used (200-1100 nm). Also, the magnetic moment of 4.81 B.M is within the range reported for a high-spin octahedral geometry around the Co(II) ion[26].

Table 5. Magnetic moments and electronic spectral data in DMSO solution for the complexes.

Complex	μ_{eff} / B.M	Charge transfer bands / cm^{-1}	*d-d* transition bands / cm^{-1}	Proposed structure
$[Co(ur)(asn)(H_2O)_2]Cl$	4.81	23585	18248, 14534	Octahedral
$[Ni(ur)(asn)(H_2O)_2]Cl$	2.9	24510	22727, 16181, 14619	Octahedral
$[Cu(ur)(asn)(H_2O)_3]Cl$	1.84	22727	16026	Distorted octahedral

$[Ni(ur)(asn)(H_2O)_2]Cl$ complex has a magnetic moment of 2.9 B.M, which is within the range reported for an octahedral geometry around the Ni(II) ion with a $^3A_{2g}$ ground term[27]. In addition, this complex has three bands in the UV-VIS spectrum (Figure 7): the band at 22727 cm^{-1} may be attributed to $^3A_{2g}\rightarrow{}^3T_{1g}$ (υ_3); 16181 cm^{-1} due to $^3A_{2g}\rightarrow{}^3T_{1g}$ (υ_2) and υ_1 at 14619 cm^{-1} in accordance with an

Eclética Química Journal, vol. 43, n. 4, 2018, 11-24
ISSN: 1678-4618
DOI: 10.26850/1678-4618eqj.v43.4.2018.p11-24

octahedral structure around the Ni(II) ion (Fig. 5a)[25, 28]. The electronic spectrum of $[Cu(ur)(asn)(H_2O)_3]Cl$ (Fig. 5b and Fig. 8) shows a strong band at 16026 cm^{-1}. This band is due to $^2E_g \rightarrow {}^2T_{2g}$ transition and a distorted octahedral geometry is suggested[25]. The broadness of this band may be due to Jahn-Teller effect[25], which confirms the distorted octahedral geometry. The magnetic moment value (1.84 B.M) is also within the range reported for the d^9-system containing one unpaired electron[29]. The bands at 23585 cm^{-1}, 24510 cm^{-1} and 22727 cm^{-1} should be attributed to the charge transfer transitions in the complexes $[Co(ur)(asn)(H_2O)_2]Cl$, $[Ni(ur)(asn)(H_2O)_2]Cl$ and $[Cu(ur)(asn)(H_2O)_3]Cl$, respectively[30].

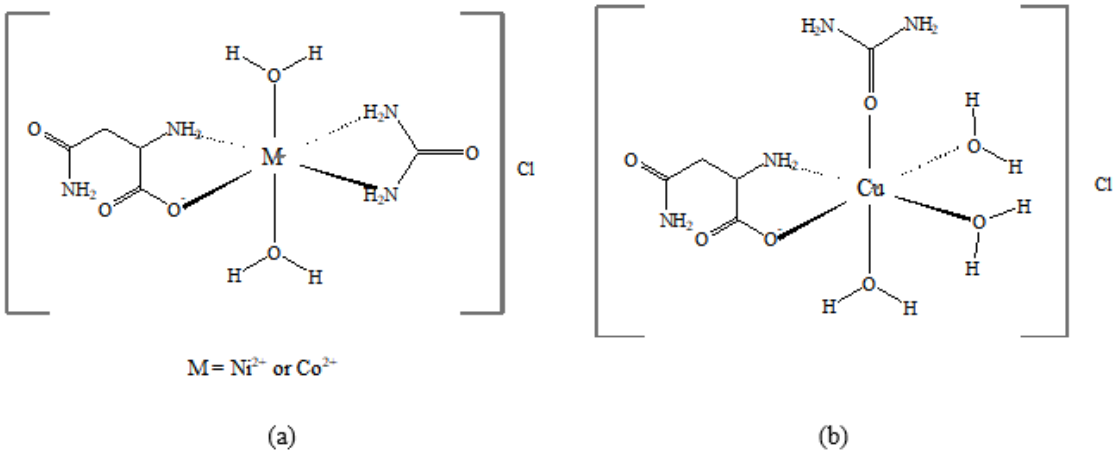

Figure 5. Suggested structure of the complexes.

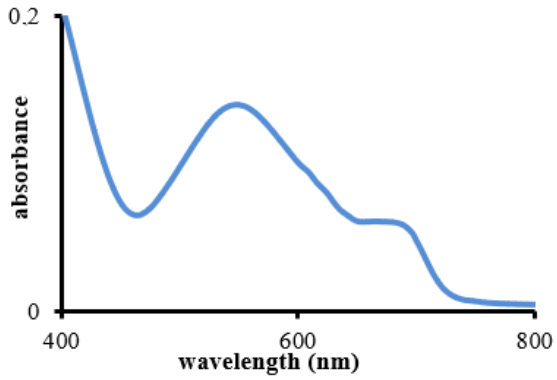

Figure 6. UV-VIS spectrum of $[Co(ur)(asn)(H_2O)_2]Cl$ complex in DM.

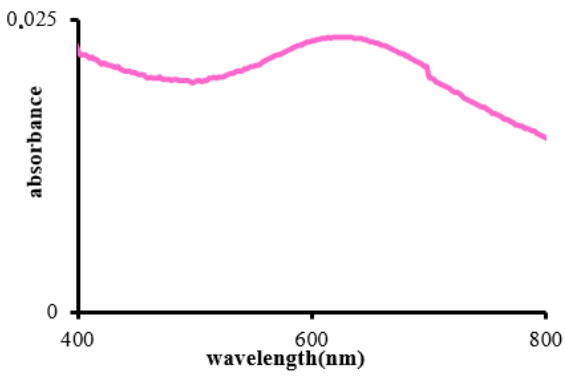

Figure 8. UV-VIS spectrum of $[Cu(ur)(asn)(H_2O)_3]Cl$ complex in DMSO solution.

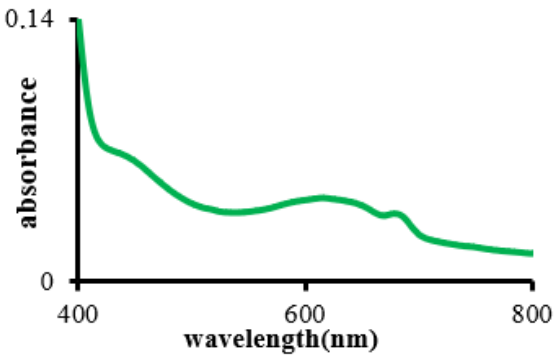

Figure 7. UV-VIS spectrum of $[Ni(ur)(asn)(H_2O)_2]Cl$ complex in DMSO solution.

4.5 The Thermal degradation study

The TGA and DTA curves of the prepared Ni and Cu complexes are given in Figures 9 to 12. These curves characterize and compare the thermal degradation of these two complexes at 10 °C min^{-1} heating rate, under nitrogen and between 20-800 °C. For the evaluation of the thermal degradation kinetics parameters at a single heating rate (10 °C min^{-1}), the activation energy (E_a) and pre-exponential factor (Z) are determined by using the Coats-Redfen method for the reaction order $n \neq 1$. When the Coats-Redfern method is

Eclética Química Journal, vol. 43, n. 4, 2018, 11-24
ISSN: 1678-4618
DOI: 10.26850/1678-4618eqj.v43.4.2018.p11-24

linearized for a correctly-chosen order of reaction (n) yields the activation energy (E_a) from the slope of the equation:

$$\log\left[\frac{1-(1-\alpha)^{1-n}}{T^2(1-n)}\right] = \log\left[\frac{ZR}{qE_a}\left(1-\frac{2RT}{E_a}\right)\right] - \frac{E_a}{2.303RT} \quad for \;\; n \neq 1$$

where: α = fraction of weight loss, T = temperature (K), Z = pre-exponential factor, R = molar gas constant, q = heating rate and n = reaction order estimated by Horovitz-Metzger method.

The thermodynamic parameters of the thermal degradation step: enthalpy (ΔH*), entropy (ΔS*), and Gibbs energy (ΔG*) of activation are calculated using the following standard equations:

$$\Delta S^* = R\ln\frac{Zh}{kT_{max}}$$

$$\Delta H^* = E_a - RT_{max}$$

$$\Delta G^* = \Delta H^* - T_{max}\Delta S^*$$

The characteristics of the thermal degradation of these two complexes recorded on the TG/DTG/DTA curves, their kinetics and thermodynamics parameters extracted from these curves are given in Tables 6-9.

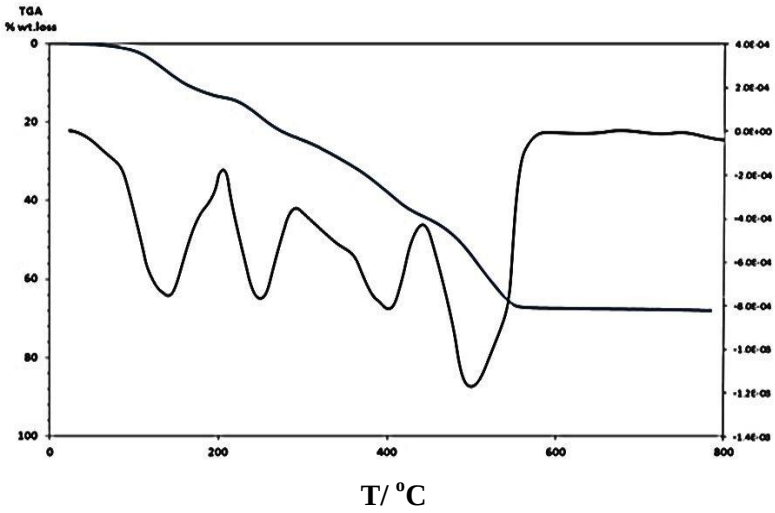

Figure 9. TG and DTG curves of [Ni(ur)(asn)(H_2O)$_2$]Cl complex.

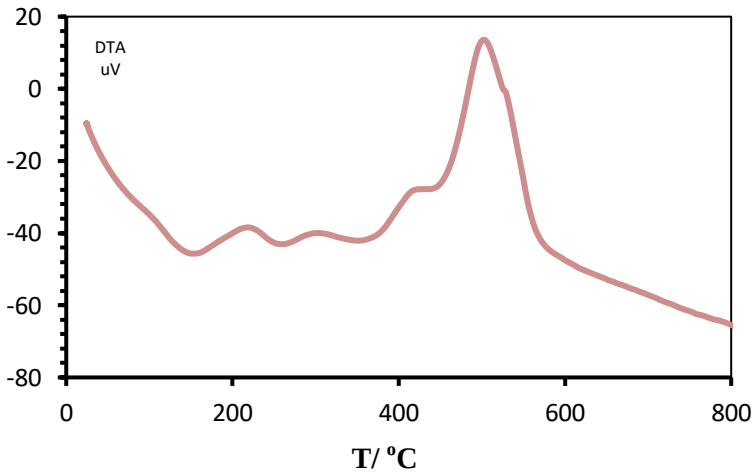

Figure 10. DTA curve of [Ni(ur)(asn)(H_2O)$_2$]Cl complex.

Eclética Química Journal, vol. 43, n. 4, 2018, 11-24
ISSN: 1678-4618
DOI: 10.26850/1678-4618eqj.v43.4.2018.p11-24

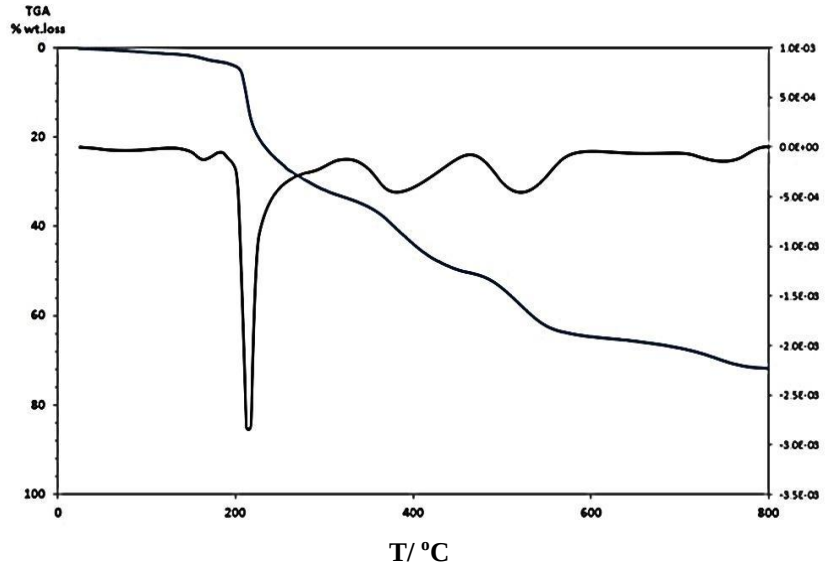

Figure 11. TG and DTG curves of $[Cu(ur)(asn)(H_2O)_3]Cl$ complex.

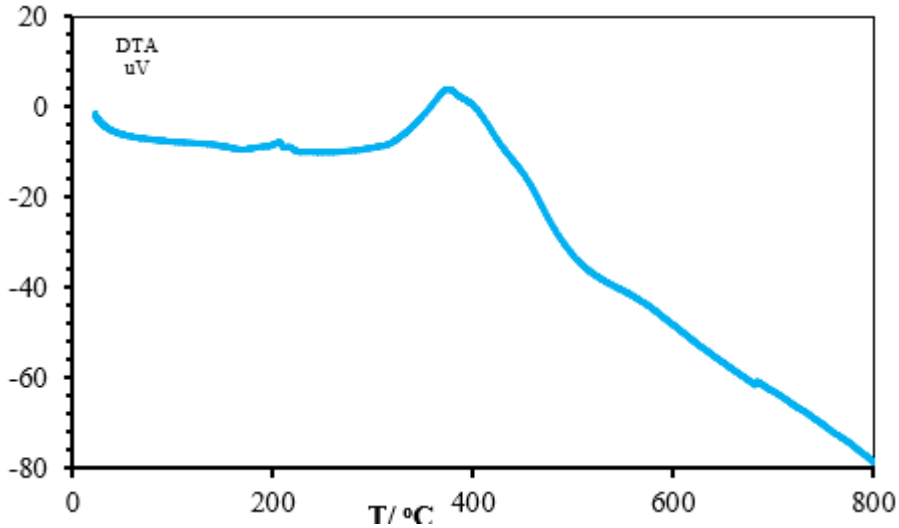

Figure 12. DTA curve of $[Cu(ur)(asn)(H_2O)_3]Cl$ complex.

4.5.1 Thermal analysis of $[Ni(ur)(asn)(H_2O)_2]Cl$

The thermolysis of $[Ni(ur)(asn)(H_2O)_2]Cl$ (Tables 6 and 7) and (Figures 9 and 10) involves several successive steps at 24-186, 186-274, 274-351, 351-428 and 428-552 °C. The first step represents the elimination of 100% coordinated H_2O molecules and 12.5% of a chloride atom (calc. 12.59%, found 12.58%) with activation energy E_a = 93 kJ mol^{-1} and a T_{DTG} peak at 132 °C. The second step corresponds to the loss of the remaining 87.5% Cl atom (calc. 12.12%, found 12.11%) which has E_a of 124 kJ mol^{-1} with T_{DTG} at 242 °C and exothermic peak T_{DTA} at 248 °C. According to the DTG curve (Figure 8), the third step is assigned to the removal of 42.86% urea molecule (calc. 8.01%, found 8.00%) and with E_a and reaction order (n) of 114 kJ mol^{-1} and 0.1, respectively. The fourth step which corresponds to the loss of the remaining urea molecule and 3.52% of asparagine (calc. 12.12%, found 12.11%) has E_a = 129 kJ mol^{-1}. The final step corresponds to the 59.82% loss of asparagine (calc. 24.41%, found 24.44%) with E_a = 131 kJ mol^{-1} and a T_{DTG} peak at 491 °C. The final residue is NiO and carbon (2.67%) as ash (O=12.2%asn, C=24.46%asn) (calc. 33.21%, found 33.21%). The values of ΔS*, ΔH* and ΔG* are: -12.4, -117.9, -165, -120.4 and -144.5 J K^{-1} mol^{-1}; 91.9, 122, 111.3, 125.7 and 126.9 kJ mol^{-1}; and 93.5, 150.5, 164.3, 172.8 and 197.8 kJ mol^{-1}, respectively, for the steps observed in the thermal decomposition of the complex.

Eclética Química Journal, vol. 43, n. 4, 2018, 11-24
ISSN: 1678-4618
DOI: 10.26850/1678-4618eqj.v43.4.2018.p11-24

Table 6. Characteristic parameters of thermal decomposition (10 °C min^{-1}) for $[Ni(ur)(asn)(H_2O)_2]Cl$.

Comp.	Steps	TGA				DTA		mass loss
		Δm % found (calc.)	T_i/°C	T_f/°C	T_{DTG}	T_{DTA}	Heat	
$[Ni(ur)(asn)(H_2O)_2]Cl$	1	12.58 (12.59)	24	186	132	134	endo	-[100%H_2O+12.5% Cl]
	2	9.66 (9.66)	186	274	242	248	exo	-[87.5% Cl]
	3	8.00 (8.01)	274	351	321	321	exo	-[42.86% ur]
	4	12.11 (12.12)	351	428	391	408	exo	-[57.14% ur+3.52% asn]
	5	24.44 (24.41)	428	552	491	500	exo	[59.82% asn]
Final residue NiO +2.67C (O=12.2%asn, C=24.46%asn): 33.21% (33.21%)								

Table 7. Kinetic and thermodynamic parameters of the thermal decomposition of $[Ni(ur)(asn)(H_2O)_2]Cl$.

Comp.	Steps	r	*n*	Z / s^{-1}	T_{max} / K	E_a / kJ mol^{-1}	Δ*S** / J K^{-1} mol^{-1}	Δ*H** / kJ mol^{-1}	Δ*G** / kJ mol^{-1}
$[Ni(ur)(asn)(H_2O)_2]Cl$	1	0.9794	2.6	$6.2x10^{11}$	132	93	-12.4	91.9	93.5
	2	0.9447	0.9	$3.5x10^{6}$	242	124	-117.9	122	150.5
	3	0.9998	0.1	$1.6x10^{4}$	321	114	-165	111.3	164.3
	4	0.9975	4.9	$4.2x10^{6}$	391	129	-120.4	125.7	172.8
	5	0.9974	2.8	$2.9x10^{5}$	491	131	-144.5	126.9	197.8

r = correlation coefficient of the linear plot, n = order of reaction, Z = pre-exponential factor.

Eclética Química Journal, vol. 43, n. 4, 2018, 11-24
ISSN: 1678-4618
DOI: 10.26850/1678-4618eqj.v43.4.2018.p11-24

Table 8. Characteristic parameters of thermal decomposition (10 °C min^{-1}) for [Cu(ur)(asn)(H_2O)$_3$]Cl.

Comp.	Steps	TGA				DTA		mass loss
		Δm % found (calc.)	T_i/°C	T_f/°C	T_{DTG}	T_{DTA}	Heat	
[Cu(ur)(asn)(H_2O)$_3$]Cl	1	2.98 (2.99)	22	178	143	168	endo	-[19.05% H_2O]
	2	29.35 (29.35)	178	306	211	207	exo	-[80.95%H_2O+100%Cl + 36.36% ur]
	3	17.35 (17.37)	306	449	362	376	exo	-[63.64% ur+16.46% asn]
	4	16.44 (16.46)	449	666	514	-	-	-[43.20% asn]
	5	5.51 (5.49)	666	785	725	-	-	-[14.40% asn]
Final residue CuO + 1.5% C (O=12.2% asn, C=13.74% asn): 28.37% (28.34%)								

Table 9. Kinetic and thermodynamic parameters of the thermal decomposition of [Cu(ur)(asn)(H_2O)$_3$]Cl.

Comp.	Steps	r	*n*	Zvz / s^{-1}	T_{max} / K	E_a / kJ mol^{-1}	Δ*S** / J K^{-1} mol^{-1}	Δ*H** / kJ mol^{-1}	Δ*G** / kJ mol^{-1}
[Cu (ur)(asn)(H_2O)$_3$]Cl	1	0.9916	4.8	2.4x10^8	143	98	-192.6	96.8	124.3
	2	0.9689	5	1.9x10^7	211	119	-102.7	117.2	138.7
	3	0.9855	2.2	3.8x10^8	362	134	-82.3	135	165.2
	4	0.9946	3.5	2.7x10^6	514	123	-126.3	118.7	183.6
	5	0.9972	4.9	3.2x10^5	725	137	-146.9	134	240.5

r = correlation coefficient of the linear plot, *n* = order of reaction, *Z* = pre-exponential factor.

4.5.2 Thermal analysis of [Cu(ur)(asn)(H_2O)$_3$]Cl

The TG and DTG curves of [Cu(ur)(asn)(H_2O)$_3$]Cl (Tables 8 and 9) and (Figures 11 and 12) show five steps of a continuous mass loss with DTG peaks indicating slow mass losses. The first step (22-178 °C) at T_{DTG} 143 °C is attributed to the release of 19.05% of coordinated H_2O (calc. 2.99%, found 2.98%). The remaining loss of H_2O, and the loss of 100% Cl and 36.36% of urea occur in the second step (178-306 °C). Third (306-449 °C), fourth (449-666 °C) and fifth (666-785 °C) steps are due to the release of [63.64%ur+16.46%asn], [43.20%asn] and [14.40%asn] fragments (calc. 17.37%, found 17.35%; calc. 16.46%, found 16.44% and calc. 5.49%, found 5.51%), respectively, at the T_{DTG} peaks at 362, 514 and 725 °C (Figure 9), respectively. The E_a calculated of these five steps are 98, 119, 134, 123 and 137 kJ mol^{-1}, respectively, and the values of ΔS*, ΔH* and ΔG* are: -192.6, -102.7, -82.3, -126.3 and -146.9 J K^{-1} mol^{-1}; 96.8, 117.2, 135.0, 118.7 and 134.0 kJ mol^{-1}, and 124.3, 138.7, 165.2, 183.6 and 240.5 kJ mol^{-1}, respectively, for the steps observed in the thermal decomposition of the complex.

4.5.2 General remarks of thermal degradation:

1. Thermal analysis confirms the presence of coordinated water molecules.

Eclética Química Journal, vol. 43, n. 4, 2018, 11-24
ISSN: 1678-4618
DOI: 10.26850/1678-4618eqj.v43.4.2018.p11-24

2. Sharp peak in Ni-complex means that the leaving parts move away faster than that in Cu-complex.
3. The releasing of the urea ligand before asparagine ligand may be due to non-ionic bonding of this ligand with the metal ions.
4. The first step which represents the dehydration of coordinated water is faster in Ni complex (E_a = 93 kJ mol^{-1}) than in Cu complex (E_a = 98 kJ mol^{-1}) (Figure 11a). The Cu complex is more stable than Ni complex (Figure 11b), which is indicated by the higher T_{max} value.
5. The chloride evolution starts at the first step in Ni complex and in the second step the Cu complex, in accordance with literature[31]. On the other side, the high value of T_{DTG} (211 °C) of Cu complex reflects its higher stability compared to Ni complex of T_{DTG} (132 °C).
6. Ni complex has a faster complete decomposition of its backbone (E_a = 131 kJ mol^{-1}) than Cu complex (E_a = 137 kJ mol^{-1}), making clear the higher stability of Cu complex.
7. The values of ΔG* for a given complex, generally, increase significantly for the subsequent decomposition steps, consequence of the increase of TΔS* values from one step to another which exceed the ΔH* values.

4. Conclusions

In this paper, some new complexes containing urea and asparagine ligands were prepared and characterized. The complexes have the following molecular formulae: $[M(L_1)(L_2)(H_2O)_n]Cl$ where M = Co(II), Ni(II) and Cu(II), L_1 = urea, and L_2 = asparagine. These complexes were characterized by elemental analysis, conductance measurements, IR, ^{1}HNMR and mass spectroscopy. Electronic spectra and magnetic measurements suggested an octahedral geometry for the complexes. Thermal analysis study showed faster decomposition reactions of the Ni complex and higher thermal stability of Cu complex.

5. Acknowledgments

This work was supported by Sana'a University, Faculty of Science. Authors extend the thanks to Inorganic Chemistry Section for using their Laboratory.

6. References

[1] Singh, M. K., Laskar, R., Sutradhar, S., Paul, B., Bhattacharjee, S., Das, A., Synthesis and Characterization of mixed ligand complexes of Co (II) ion with some N and S donor, IOSR Journal of Applied Chemistry 7 (4) (2014) 24-29. https://doi.org/10.9790/5736-07412429.

[2] Bindu, G. H., Rao, G. N., Mixed ligand complexes of essential metal ions with L-glutamine and succinic acid in sodium dodecyl sulfate–water mixtures, J. Serb. Chem. Soc. 77 (4) (2012) 453–463. https://doi.org/10.2298/JSC110201177B.

[3] Li, Y. T., Yan, C. W., Zhu, Y., Guan, H. S., Synthesis and Magnetic Studies of M-Oxamidobridged Copper (II)–Manganese (II) Heterobinuclear Complexes, Synth. React. Inorg., Met-Org. Nano-Met. Chem. 34 (2005) 1165–1179. https://doi.org/10.1081/SIM-120039264.

[4] Aydogdu, Y., Yakuphanoglu, F., Aydogdu, A., Cukurovah, E., Solid State Electrical Conductivity Properties of Copper Complexes of Novel Oxime Compounds Containing Oxolane Ring, Material Letters 57 (2003) 3755-3760. https://doi.org/10.1016/S0167-577X(03)00174-5.

[5] Rahaman ,S. K. H., Fun, H. K., Ghosh, B. K., A Study on Copper(II)-Schiff Base-Azide Coordination Complexes: Synthesis, X-Ray Structure and Luminescence Properties of [Cu(L)(N3)]X (L = Schiff Bases; X = ClO4, PF6), Polyhedron 24 (2005) 3091-3097. https://doi.org/10.1016/j.poly.2005.06.028.

[6] Carballo, R., Castineiras, A., Covelo, B., Martinez, E. G., Niclós, J., Lopez, E. M. V., Solid state coordination chemistry of mononuclear mixed ligand complexes of Ni (II), Cu (II) and Zn (II) with □-hydroxycarboxylic acids and imidazole, Polyhedron 23 (9) (2004) 1505-1518. https://doi.org/10.1016/j.poly.2004.02.028.

[7] S. Rafique, S., Idrees, M., Nasim, A., Akbar, H., Athar, A., Transition metal complexes as potential therapeutic agents, Biotechnol. Mol. Biol. Rev. 52 (2) (2010) 38-45.

[8] Saffran, E. K., Kinne, R. K. H., Vitalism and Synthesis of Urea - From Friedrich Wöhler to Hans A. Krebs, American Journal of Nephrol 19 (1999) 290–294. https://doi.org/10.1159/000013463.

[9] Penland, R. B., Mizushima, S., Curran, C., Quagliano, J. V., Infrared Absorption Spectra of Inorganic Coordination Complexes. X. Studies of Some Metal-Urea Complexes, J. Am. Chem. Soc. 79 (7) (1957) 1575–1578. https://doi.org/10.1021/ja01564a014.

[10] Savinkina , E. V., Golubev, D. V., Podgornov, K.V., Albov, D. V., Grigoriev, M. S., Davydova , M. N., Different Types of Coordinated Urea Molecules in its Complexes with Rare-Earth Iodides and Perchlorates, Zeitschrift für anorganische und allgemeine Chemie 1 (39) (2013) 53-58. https://doi.org/10.1002/zaac.201200267.

[11] Amenda, J. P., Helgesonb, H. C., Solubilities of The Common L-A-Amino Acids as A Function of Temperature Solution PH, Pure & Appl. Chem. 69 (5) (1997) 935-942. https://doi.org/10.1351/pac199769050935.

[12] Lea, P. J., Sodek, L., Parry, M. A. J., Shewry, P. R., Halford, N. G., Asparagine in plants, Ann. Appl. Biol. 150 (2007) 1–26. https://doi.org/10.1111/j.1744-7348.2006.00104.x.

[13] Alabdali, A. J., Ibrahim, F. M., Synthesis and Thermal Study of Co (II), Ni (II), Cu (II) Mixed Ligand Complexes Using Histidine As Tridentate Ligand, IOSR Journal of Applied Chemistry (IOSR-JAC) 6 (6) (2014) 60-63. https://doi.org/10.9790/5736-0666063.

[14] Mihsen, H. H., Shareef, N. K., Synthesis, characterization of mixed- ligand complexes containing 2,2-Bipyridine and 3-aminopropyltriethoxysilane, Journal of Physics: Conf. Series 1032 (2018) 012066. https://doi.org/10.1088/1742-6596/1032/1/012066.

[15] Leelavathy, C.1, Arul Antony, S., Structural elucidation and thermal studies of some novel mixed ligand schiff base metal (II) complexes, International Journal of Basic and Applied Chemical Sciences 3 (4) (2013) 88-95. http://www.cibtech.org/jcs.htm.

[16] Pop, V., David, L., Simuţ, C., Drăgan, S. F. M., Spectroscopic Investigation of Copper (II) Complex with Mixed Ligands, Aspartic Acid and Urea, Anal. Univ. Din Orad. 17 (2003) 17- 21. http://www.fizicaoradea.ro/docs/2003_a_2.pdf.

[17] Gamo, I., Infrared Spectra of Water of Crystallization in Some Inorganic Chlorides and Sulfates, Bull. Chem. Soc. Jpn. 34 (1430) (1961) 760-764. https://doi.org/10.1246/bcsj.34.760.

[18] Abdul-Ameer, N., Synthesis and Characterization of Mn(Π), Co(Π), Ni(Π) and Cu(Π) Complexes with Mixed Ligands, Aceturic Acid and Urea, Tikrit Journal of Pure Science 17 (2) (2012) 55-61. ISSN: 18131662.

[19] Sagatys, D. S., Bott, R. C., Smith, G., Byriel, K. A., Kennard, C. H. L , The Preparation and Crystal Structure of A Polymeric (1:1)-Silver Nitrate-Urea Complex, $[(AgNO_3)2(CH_4N_2O)2]N$, Polyhedron 11 (1) (1992) 49-52. https://doi.org/10.1016/S0277-5387(00)83258-1.

[20] Bellamy, L. J., The Infrared Spectra of Complex Molecules, 3rd Ed., London: Chapman and Hall, 1975.

[21] El-Metwally, N. M., Gabr, I. M., El-Asmy, A. A., Abou-Hussen, A. A., Spectral, Magnetic, Electrical and Thermal Studies on Malonyl Bis(Thiosemicarbazide) Complexes, Transition Metal Chemistry 31 (1) (2006) 71-78. https://doi.org/10.1007/s11243-005-6347-6.

[22] Gaballa, A. S., Teleb, S. M. Nour, E.-M., Synthesis and Spectroscopic Studies of Metal Complexes Formed in The Reaction of Metal Ions with Urea At High Temperature, Journal of The Korean Chemical Society 51 (4) (2007) 339-345. https://doi.org/ 10.5012/jkcs.2007.51.4.339.

[23] Amparo, C., Virtudes, M., Eiles, M., Carles, M., Methionine and Histidine Pd(II) and Pt(II) Complexes: Crystal Structures and Spectroscopic Properties, J. Inorg. Biochem. 48 (1992)135-152. https://doi.org/10.1016/0162-0134(92)80023-O.

[24] Hosny, W. M., Dioxouranium(VI) Mixed Ligand Complexes Containing 8-Hydroxyquinoline and Some Amino Acids, Synth. React. Inorg. Met. Org.Chem. 2 (1998) 1029-1052. https://doi.org/10.1080/00945719809351686.

[25] El-Asmy, A. A., Khalifa, M. E., Rakha, T. H., Hasanian, M. M., Abdallah, A. M., Mono and

trinuclear complexes of oximinoacetoacetyl-pyridine-4-phenylthiosemicarbazone, Chem. Pharm. Bull. 48 (2000) 41-44. https://doi.org/10.1248/cpb.48.41.

[26] Saha, N. C., Butcer, R. J., Chaudhuri, S., Saha, N., Synthesis and spectroscopic characterisation of cobalt (III) and nickel (II) complexes with 5-methyl-3-formylpyrazole-N (4)-dibutylthiosemicarbazone (HMP z NBu 2): X-ray crystallography of [Co (MPz NBu 2)2] NO3· H2O (I) and [Ni (HMPz NBu2)2](ClO4)2 (II), Polyhedron 22 (3) (2003) 383-390. https://doi.org/10.1016/S0277-5387(02)01343-8.

[27] El-Metwally, N. M., El-Asmy, A. A., Chelating Activity of Bis(Diacetylmonoxime) Thiocarbohydrazone Towards VO2+, Co(II), Ni(II), Cu(II) and Pt(IV) Ions, Journal of Coordination Chemistry 59 (14) (2006) 1591-1601. https://doi.org/10.1080/00958970600572743.

[28] B.N.Figgis, "Introduction To Ligand Field Theory", Interscience, New York, 258, 319(1967).

[29] A.B.P. Lever, Inorganic Electronic Spectroscopy, Elsevier, Amsterdam (1968).

[30] Al-Maydama, H., El-Shekeil, A., Khalid, M. A., Al-Karbouly, A., Thermal degradation behaviour of some polydithiooxamide metal complexes, Eclét. Quím. 31 (1) (2006) 45-52. https://doi.org/10.1590/S0100-46702006000100006.

[31] Komiyama, T., Igarashi, S., Yukawa, Y., Synthesis of polynuclear complexes with an amino acid or a peptide as a bridging ligand, Current Chemical Biology 2 (2) (2008) 122-139. https://doi.org/10.2174/187231308784220509.

Eclética Química Journal

Original article
iq.unesp.br/ecletica

| Vol. 43 | n. 4 | 2018 |

Physicochemical and biological activity studies on complexes of some transition elements with mixed ligands of glycine and urea

Maher Ali Al-Maqtari[1+], Mohammed Kassem Al-Qadasy[1], Yasmin Mosa'd Jamil[1], Fathi Mohammed Al-Azab[1], Amani A. Al-Gaadbi[1]

[1] Sana'a University, Faculty of Science, Chemistry Department, Sana'a, Yemen

[+] Corresponding author: Maher Ali Al-Maqtari, e-mail address: al.maqtarimaher@yahoo.com

ARTICLE INFO

Article history:
Received: August 8, 2018
Accepted: November 11, 2018
Published: December 5, 2018

Keywords:
1. urea
2. glycine
3. transition elements
4. complexes

ABSTRACT: The reaction of urea (ur) and glycine (gly) with the metal ions Co(II), Ni(II) and Cu(II) in ethanolic solution of 1M:1L_1:1L_2 molar ratio (where M= Co(II), Ni(II) and Cu(II), and L_1 = urea L_2 = glycine) led to the preparation of complexes of the general formula $[M(ur)(gly)(H_2O)_2]Cl$. Elemental microanalysis (CHN), molar conductivity measurements, IR,^{1}HNMR, Mass and UV-VIS spectroscopic, and magnetic susceptibility measurements were used for the characterization of the compounds. Thermal analyses were used for the complexes degradation characterization. The complexes have an octahedral geometry and are of electrolytic nature in DMSO solvent with the absence of inner-sphere coordination of the chloride anion. An inhibition zone was observed for Ni-urea-glycine complex against *Escherichia coli* when the biological activity was considered.

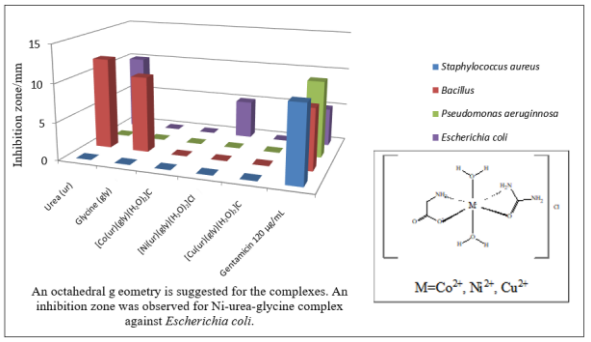

1. Introduction

The synthesis and study of mixed ligand transition metal complexes have been of growing interest[1, 2]. New materials with useful properties such as electrical conductivity photoluminescence, magnetic exchange, nonlinear optical property and antimicrobial activity can be provided by using mixed ligand transition metal complexes[3-5].

Urea ($CO(NH_2)_2$) plays an important role in many biological processes such as decomposition of proteins and amino acids catabolism. In 1828, Wöhler discovered urea, when organic materials were prepared from inorganic substances.

All living things contain building blocks of amino acids[6], which were first discovered as constituents of natural products and then observed to be the major components of proteins.

All life forms on earth consist of the simplest proteinaceous amino acid, called glycine or amino acetic acid[7]. Glycine is a neutral, aliphatic, optically inactive nonessential amino acid[8] and it is the only protein amino acid that does not have optical isomers[9]. Most of the metal ions form mono, bis and tris complexes with glycine that acts as a bidentate ligand forming stable 5-membered chelating rings via the N atom of the amino group and O atom of carboxylate group[10].

The mixed ligand complexes of urea and glycine acid with Co(II), Ni(II) and Cu(II) ions were synthesized, characterized and thermally studied for the first time in this work.

2. Materials and methods

2.1 Materials

CC BY

All Chemical reagents used were purchased from BDH and used as provided.

2.2 Synthesis of the complexes

Generally, the solid complexes were prepared by the same methodology previously described[11]. Briefly, an ethanolic solution of hydrated metal chloride (0.01 mol) was dropwise added in an ethanolic solution of the first ligand (urea 0.01 mol) with stirring. The mixture was refluxed for 12 h with constant stirring. A hot solution of 0.01 mol glycine in 1:1 ethanol / water mixture ratio was dropwise added to the urea / metal mixture and drops of 1 mol L^{-1} NaOH solution were used to adjust pH 7.0 - 7.5 to deprotonate NH_3^+ of the glycine to NH_2. The mixture was refluxed for 2 h until resulting in the formation of a colored precipitate. The resulting product was filtered off and then washed with distilled water to remove NaCl. The product was further washed with absolute ethanol/dimethylformamide (DMF) and left to dry. Acceptable yield percentage was obtained (52-66%).

2.3 Instrumentation

Glass capillary tubes were used to measure the melting points of the metal complexes in degrees celsius on a Stuart Scientific electrothermal melting point apparatus. Silica Gel GF_{254} plates (mn-kieselgel G., 0.2 mm thickness) was used for TLC. Vario ELFab instrument was used for elemental analysis (carbon, hydrogen and nitrogen) of complexes. Chloride was volumetrically or gravimetrically determined by silver nitrate. The amount of water was determined gravimetrically using weight loss method and also from thermal analysis. Perkin-Elmer 2380 flame atomic absorption spectrophotometer was used to measure the metal content. Jenway conductivity meter model 4510 was used to measure the molar conductance of 10^{-3} mol L^{-1} solutions of the metal complexes in dimethylsulfoxide (DMSO) solvent. IR spectra of the metal complexes were measured by using FT/IR-140 (Jasco, Japan). A Varian FT-300 MHz spectrometer in d_6-DMSO solvent was used for obtaining proton ^{1}HNMR spectra, using TMS as internal standard. Mass spectra were recorded on a JEOL JMS600 spectrometer. The electronic spectra of the complexes were measured in the range 400-800 nm using an UV–VIS spectrophotometer Specord 200, Analytilk Jena (Germany). The mass susceptibility (χ_g) of the solid complexes was measured at room temperature using Gouy's method on a magnetic susceptibility balance from Johnson Metthey and Sherwood model. Differential Thermal Analysis (DTA) and Thermogravimetric Analysis (TGA) were performed using the Shimadzu DTA-50 and Shimadzu TGA-50H thermal analyzers. The experiments were carried out in the temprature range from 25 to 800 ^oC under nitrogen atmosphere in a platinum pan, heating rate of 10 ^oC / min and flow rate of 30 mL min^{-1}. The antibacterial activity against four species of bacteria (*Staphylococcus aureus*, *Bacillus* spp., *Escherichia coli* and *Pseudomonas aeruginosa*) was tested by agar diffusion method. 1000 µg mL^{-1} concentration for each of these compounds were individually prepared in DMSO, then the filter paper disc (whatman No.1.5 mm diameter) was saturated with the solution of these compounds. The discs were placed on the surface of Millar Hinton agar dishes seeded with the strains of bacteria. The inhibition zones (mm) were measured after 24 h at 37 ^oC. DMSO and gentamicin (120 µg mL^{-1}) were used as control and reference, respectively.

3. Results and discussion

Complexes of Co(II), Ni(II) and Cu(II) with urea (ur) and glycine (gly) ligands have been prepared and characterized. Analytical data, physical properties, molar conductivity, and composition of the synthesized complexes are given in Tables 1 and 2. The molar conductivity values (135-149 S cm^2 mol^{-1}) reflect the electrolytic properties of these complexes. The single spot appearance in the TLC proves the purity of these complexes.

Eclética Química Journal, vol. 43, n. 4, 2018, 25-36
ISSN: 1678-4618
DOI: 10.26850/1678-4618eqj.v43.4.2018.p25-36

Table 1. Some physical properties of the complexes.

Complex Proposed Formula	Color	M.p /°C	TLC		molar conductivity Λ_m / S cm^2 mol^{-1}
			No.of spots	Rf	
$[Co(ur)(gly)(H_2O)_2]Cl$ $[Co(C_3H_{12}N_3O_5)]Cl$	dark violet	>350	One	0.28	149
$[Ni(ur)(gly)(H_2O)_2]Cl$ $[Ni(C_3H_{12}N_3O_5)]Cl$	pale green	226±1	One	0.39	135
$[Cu(ur)(gly)(H_2O)_2]Cl$ $[Cu(C_3H_{12}N_3O_5)]Cl$	light blue	>350	One	0.39	148

Table 2. Elemental analysis of the complexes.

Complex proposed formula	Molar mass		Elemental analysis									
			%C		%H		%N		%M		%Cl	
	calc.	found	calc.	found	calc.	found	calc.	found	calc.	found	calc.	found
$[Co(ur)(gly)(H_2O)_2]Cl$ $[Co(C_3H_{12}N_3O_5)]Cl$	264.53	264.03	13.62	13.65	4.57	4.58	15.89	15.91	22.28	22.32	13.40	13.45
$[Ni(ur)(gly)(H_2O)_2]Cl$ $[Ni(C_3H_{12}N_3O_5)]Cl$	264.29	264.34	13.63	13.63	4.58	4.58	15.90	15.90	22.21	22.20	13.41	13.43
$[Cu(ur)(gly)(H_2O)_2]Cl$ $[Cu(C_3H_{12}N_3O_5)]Cl$	269.14	269.19	13.38	13.39	4.49	4.49	15.61	15.61	23.61	23.61	13.17	13.17

3.1 IR spectra of urea - glycine complexes

The coordination sites of urea and glycine ligands in their complexes were investigated. The infrared spectra show that urea acts as a neutral bidentate ligand through C=O and NH_2 groups while glycine behaves as a bidentate anion ligand through COO^- and NH_2 groups. IR spectra of urea-glycine complexes are represented in Figures 1, 2 and 3. Assignments of the characteristic bands are summarized in Table 3. As it was postulated, the metal complexes were quite different when compared with the free ligands.

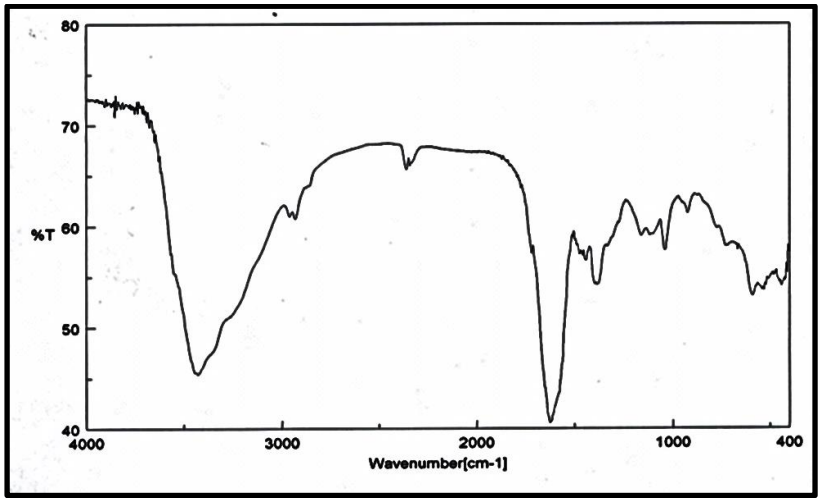

Figure 1. IR spectrum of $[Co(ur)(gly)(H_2O)_2]Cl$ complex.

Eclética Química Journal, vol. 43, n. 4, 2018, 25-36
ISSN: 1678-4618
DOI: 10.26850/1678-4618eqj.v43.4.2018.p25-36

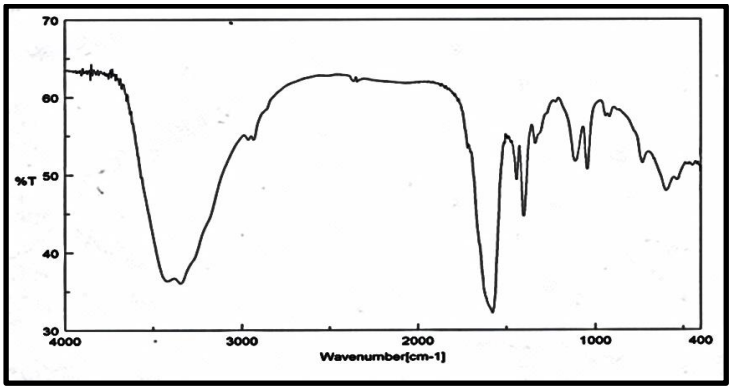

Figure 2. IR spectrum of $[Ni(ur)(gly)(H_2O)_2]Cl$ complex.

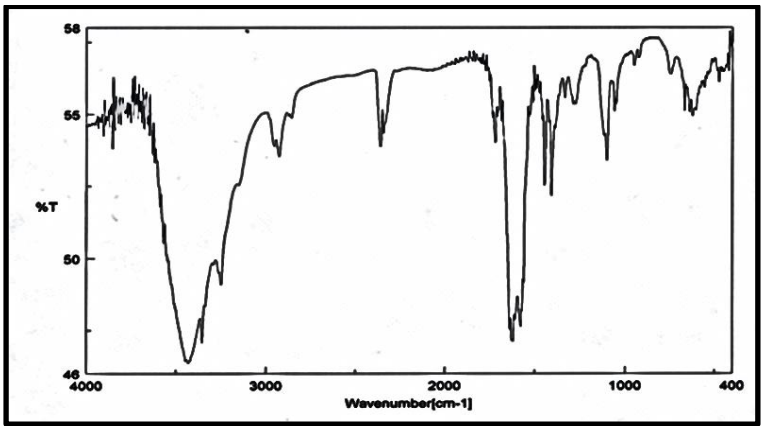

Figure 3. IR spectrum of $[Cu(ur)(gly)(H_2O)_2]Cl$ complex.

Eclética Química Journal, vol. 43, n. 4, 2018, 25-36
ISSN: 1678-4618
DOI: 10.26850/1678-4618eqj.v43.4.2018.p25-36

Table 3. Main IR bands (cm^{-1}) of the urea-glycine complexes

Urea	Glycine	$[Co(ur)(gly)(H_2O)_2]Cl$	$[Ni(ur)(gly)(H_2O)_2]Cl$	$[Cu,(ur)(gly)(H_2O)_2]Cl$	Assignment
-	3164-3007br	-	-	-	$\upsilon(NH_3^+)$
3353m	-	ur-3250br gly-3185w,br	ur-3270br gly -3168w,br	ur -3248br gly -3160br	$\upsilon_s(NH_2)$
3466 m	-	ur, gly - 3376br	ur,gly – 3346m	ur - 3355 m gly -3290w	$\upsilon_{as}(NH_2)$
1618br	-	-	-	1609w	δ (NH)
-	1410m	1397 m	1402s	1408s	$\upsilon_s(COO^-)$
-	1598br	1509w	1578s	1578m	$\upsilon_{as}(COO^-)$
1695w	1715w	ur – 1625s gly –1718m	ur – 1680w gly –1718w	ur - 1618 m gly–1719m	$\upsilon(CO)$
1468br	1033s	ur – 1474w gly -1040m	ur – 1475w gly -1045m	ur–1475w gly –1050 w	$\upsilon(CN)$
-	2892br	2885br	2863 w.br	2857br	$\upsilon(CH_2)$
-	1442m	1439m	1441s	1446s	δ (CH_2)
-	-	3431br	3422br	3432br	H_2O $\upsilon(OH)$
-	-	451w	483 w	475 w	$\upsilon(M-O)$
-	-	440w	460 w	421 w	$\upsilon(M-N)$

s = strong, m = medium, br = broad, w = weak, w,br = weak and broad

The infrared spectral data of the complexes are as follows:

(1) All the complexes spectra show a broad band at 3422-3432 cm^{-1} that corresponds to the stretching mode of water existing in the complexes as identified by thermal and elemental analysis. The coordinated water is identified by the appearance of ρ_r (rocking) and ρ_w (wagging) at 925 cm^{-1} and 511 cm^{-1}, respectively[12].

(2) The amino groups of urea show lower-shift of 123-103 cm^{-1} and of 120-90 cm^{-1} for symmetrical and asymmetrical stretching $\upsilon(NH_2)$ frequencies, respectively. This strongly suggests that the nitrogen atom of amino group must be involved in complexation, and the appearance of a new band in the range of 406-460 cm^{-1}, assigned to $\upsilon(M-N)$ vibration, confirms this proposition[13, 14].

(3) A new band at 1680-1618 cm^{-1} is attributed to $\upsilon(CO)$ from urea, assigned to $\upsilon(C=O–M)$.

(4) The characteristic bands in complexes spectra occur in the ranges 3185-3160 cm^{-1} and 3376-3290 cm^{-1} for symmetrical and asymmetrical $\upsilon(NH_2)$ group of glycine, respectively, which appears at lower wave number than the free $\upsilon(NH_2)$. Hence, coordination through nitrogen of the amino group is involved[15].

(5) The symmetrical $\upsilon(COO^-)$ and asymmetrical $\upsilon(COO^-)$ vibrations of glycine shift by 13-8 cm^{-1} and 89-20 cm^{-1}, respectively. This confirms that carboxylate is acting as a monodentate group[16]. Glycine acts as monobasic bidentate, through the nitrogen of amino and oxygen of carboxylate groups in these complexes[17, 18].

(6) The IR spectra in the range 483-451cm^{-1} and 460-421cm^{-1} show bands of low intensity due to stretching vibrations of $\upsilon(M-O)$ and $\upsilon(M-N)$, respectively[13, 14].

3.2. ^{1}HNMR spectra of urea-glycine complexes

Complexes were investigated by using ^{1}HNMR spectra in d_6-DMSO and TMS (tetramethyl silane) as standard and data are in Table 4. $[Co(ur)(gly)(H_2O)_2]Cl$, $[Ni(ur)(gly)(H_2O)_2]Cl$ and $[Cu(ur)(gly)(H_2O)_2]Cl$ complexes show signals in the range 5.4-7.2 ppm attributed to the amide group of urea[19, 20]. The methylene group of glycine ($-CH_2-$) in Co(II), Ni(II) and Cu(II) complexes absorbs near 3.2, 3.2 and 3.1 ppm, respectively. NH_2 group shows signals at 2.9, 2.5 and 2.6 ppm, respectively[21, 22]. In urea, one amine and the carbonyl groups are coordinated to the central metal ion without displacement of NH_2 proton,

Eclética Química Journal, vol. 43, n. 4, 2018, 25-36
ISSN: 1678-4618
DOI: 10.26850/1678-4618eqj.v43.4.2018.p25-36

while in glycine presents a new signal in the range 2.5-2.9 ppm because of the deprotonation of NH^{3+} to NH_2. The appearance of a new signal around 3.5-3.8 ppm confirms the presence of water molecules in the complexes[23].

Table 4. ^{1}HNMR chemical shift (ppm) of free urea and glycine ligands and of complexes.

System	$(CH)_\alpha$ α =Alpha	NH_3^+	$NH_{2(gly)}$	$NH_{2(ur)}$	H_2O
urea	-	-	-	6-7.5	-
glycine	3.5	8-7	-	-	-
$[Co(ur)(gly)(H_2O)_2]Cl$	3.2	-	2.9	$5.4_{(bonding)}$ $6.4_{(nonbonding)}$	3.8
$[Ni(ur)(gly)(H_2O)_2]Cl$	3.2	-	2.5	$4.7_{(bonding)}$ $7.2_{(nonbonding)}$	3.7
$[Cu(ur)(gly)(H_2O)_2]Cl$	3.1	-	2.6	$5.5_{(bonding)}$ $7_{(nonbonding)}$	3.5

3.3 Mass spectra of urea-glycine complexes

The mass spectra of Co(II), Ni(II) and Cu(II) complexes with urea and glycine reveal molecular ion peaks at m/z (calc. 264.53, found 264.03 (4%)), (calc. 264.29, found 264.34 (11%)) and (calc. 269.14, found 269.19 (9%)), respectively.

The molecular ion of $[Co(ur)(gly)(H_2O)_2]Cl$ complex loses glycinate ($NH_2CH_2COO^-$) ion and $2H_2$ leaving an ion at m/z 185.67, which by its turn, loses H_2O, Cl, CO, NH_3 and H_2 giving an ion at m/z 85.01.

The mass spectrum of $[Ni(ur)(gly)(H_2O)_2]Cl$ complex exhibited a peak at m/z 244.90, indicating the loss of H_2 and NH_3, then this molecular ion loses H_2O and ½Cl_2 leaving an ion at m/z 192.83, which further loses one more $H_2NCH_2COO^-$ affording an ion at m/z 118.87. The complex $[Cu(ur)(gly)(H_2O)_2]Cl$ loses [CO, ½Cl_2] and H_2O to give ions at m/z 205.68 and 251.19, respectively.

3.4 Electronic and magnetic spectral analysis

The magnetic moments of the Co(II), Ni(II) and Cu(II) complexes as well as their electronic spectra data have provided good evidence for the structures of these complexes as shown in Table 5. $[Co(ur)(gly)(H_2O)_2]Cl$ hexa-coordination is suggested. This is based on the spectrum (Figure 5) recorded in DMSO solution which shows bands at 17985 cm^{-1} and 14482 cm^{-1}, due to transition of $^4T_{1g} \rightarrow {}^4T_{1g}(P)$ (υ3) and $^4T_{1g} \rightarrow {}^4A_{2g}$ (υ2), respectively[23]. The third band of the spectrum, assigned to υ1, could not be observed due to the limited range of the used instrument (200-1100 nm). $[Co(ur)(gly)(H_2O)_2]Cl$ has a magnetic moments of 4.76 B.M; this value is due to a high-spin octahedral geometry around the Co(II) ion as reported previously[24]. Moreover, the violet colour of octahedral Co(II) complexes is in good agreement with those previously reported[25].

Eclética Química Journal, vol. 43, n. 4, 2018, 25-36
ISSN: 1678-4618
DOI: 10.26850/1678-4618eqj.v43.4.2018.p25-36

Table 5. Magnetic moment and electronic spectral data in DMSO solution for the complexes.

complex	μ_{eff} / B.M	charge transfer bands / cm^{-1}	*d-d* transition bands / cm^{-1}	proposed structure
$[Co(ur)(gly)(H_2O)_2]Cl$	4.76	23697	17985, 14492	octahedral
$[Ni(ur)(gly)(H_2O)_2]Cl$	3.2	23419	21459, 14970, 13477	octahedral
$[Cu(ur)(gly)(H_2O)_2]Cl$	1.43	24272	12987	distorted octahedral

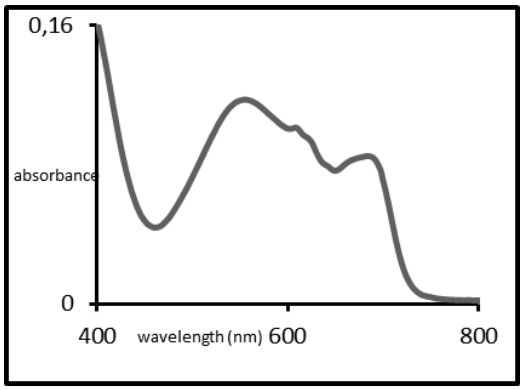

Figure 4. UV-VIS spectrum of $[Co(ur)(gly)(H_2O_2]Cl$ complex in the MSO solution.

From the above discussion (Figure 5) of $[Co(ur)(gly)(H_2O_2]Cl$ can be suggested. Furthermore, previous studies proved that the broad bands centred at 23697 cm^{-1} should be assigned to charge-transfer transitions in $[Co(ur)(gly)(H_2O)_2]Cl$[26].

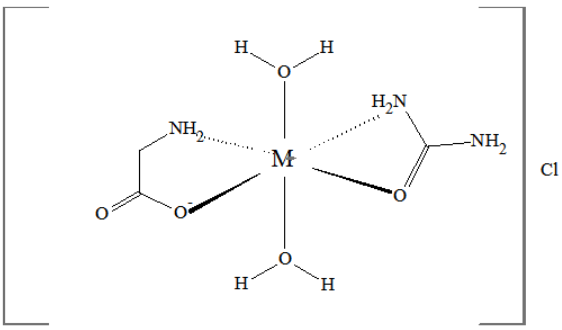

M = Ni^{2+}, Co^{2+} or Cu^{2+}

Figure 5. Suggested structure for the complex.

The magnetic moment data as well as the electronic spectrum data of the nickel complex are given in Table 5. The complex $[Ni(ur)(gly)(H_2O)_2]Cl$ has a magnetic moment value of 3.2 B.M consistent with an octahedral geometry around the Ni(II) ion with a $^3A_{2g}$ ground term, which lies in the range reported in the literature[27]. In addition, the complex has three bands in the UV-VIS recorded in DMSO solution (Figure 6): 21459 cm^{-1} may be due to the $^3A_{2g} \rightarrow {}^3T_{1g}$ (υ3); 14970 cm^{-1} due to $^3A_{2g} \rightarrow {}^3T_{1g}$ (υ2); 13477 cm^{-1} in the transition range of an octahedral structure around the Ni(II) ion (υ1) (Figure 5)[28]. The green colour is also an additional evidence for the octahedral structure[26]. The band at 23419 cm^{-1} may be attributed to the charge transfer transition of $[Ni(ur)(gly)(H_2O)_2]Cl$ complex[23].

$[Cu(ur)(gly)(H_2O)_2]Cl$ (structure in Figure 5) has an electronic spectrum (Figure 7) that shows a strong band at 12987 cm^{-1} due to $^2E_g \rightarrow {}^2T_{2g}$ transition, suggesting a distorted octahedral geometry[26]. The broadness in the band may be due to Jahn-Teller effect[29] and the proposed geometry is also supported by the blue colour of this complex[27]. The magnetic moment value of this complex 1.43 B.M agrees with the d^9 system containing one unpaired electron[26]. The observed band at 24272 cm^{-1} in the spectrum of the complex may be due to LMCT (L→M charge transfer transition) of $[Cu(ur)(gly)(H_2O)_2]Cl$ complex[30].

Eclética Química Journal, vol. 43, n. 4, 2018, 25-36
ISSN: 1678-4618
DOI: 10.26850/1678-4618eqj.v43.4.2018.p25-36

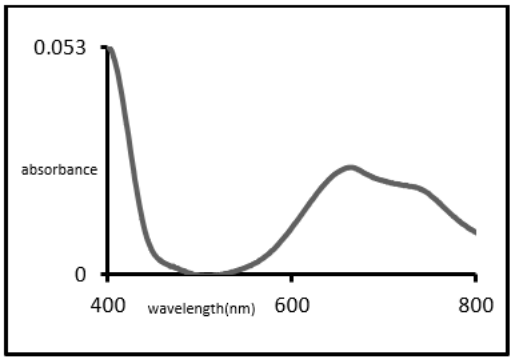

Figure 6. UV-VIS spectrum of $[Ni(ur)(gly)(H_2O)_2]Cl$ complex in DMSO solution.

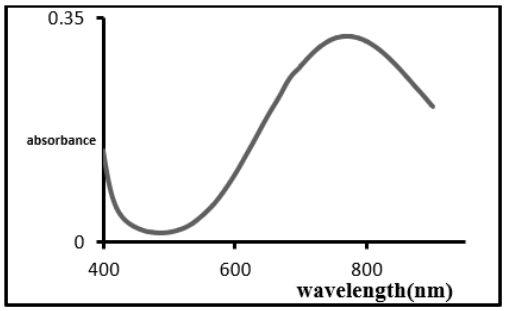

Figure 7. UV-VIS spectrum of $[Cu(ur)(gly)(H_2O)_2]Cl$ complex in DMSO solution.

3.5. Thermal analysis of Cu-urea-glycine complex

The thermal and kinetic parameters for each step in the decomposition sequences of the Cu-complex were determined by using the integral Coast-Redfern equation. The Coats-Redfern method is linearized for a correctly-chosen order of reaction (n) and the activation energy (E_a) is obtained from the slope of the log [y] *versus* T^{-1} plot from Equation:

$$log\left[\frac{1-(1-\alpha)^{1-n}}{T^2(1-n)}\right] = log\left[\frac{ZR}{qE_a}\left(1-\frac{2RT}{E_a}\right)\right] - \frac{E_a}{2.303RT} \quad for\ n \neq 1 \quad \rightarrow 1$$

where: α = fraction of mass loss, T = temperature (K), Z = pre-exponential factor, R = molar gas constant, q = heating rate and n = reaction order; estimated by Horovitz-Metzger method.

The thermodynamic parameters of the thermal degradation step: enthalpy (ΔH^*), entropy (ΔS^*), and Gibbs energy (ΔG^*) of activation are calculated using the following standard equations:

$$\Delta S^* = R\ln\frac{Zh}{kT_{max}}$$

$$\Delta H^* = E_a - RT_{max}$$

$$\Delta G^* = \Delta H^* - T_{max}\Delta S^*$$

where z, k, and h are the pre-exponential factor, Boltzmann and Planck constant, respectively.

The TG and DTA thermograms of $[Cu(ur)(gly)(H_2O)_2]Cl$ complex (Figures 8 and 9) are characterized by the three fast decomposition steps (25-318, 318-361 and 361-375 °C). The T_{DTG} at 302 °C is consistent with the evolution of 100% of coordinated water, 100% of bonded chloride and 60% the urea ligand (calc. 39.95%, found 39.93%). The activation energy calculated is 89 kJ mol^{-1} (Table 6). The remaining urea molecule may be eliminated in the second step together with 52.72% of glycine molecule (calc. and found 23.43%). In this step (318-361 ºC), the activation energy is 123 kJ mol^{-1} and the order of decomposition reaction is 3.6 with the apparent T_{DTG} (334 ºC) and the exothermic (T_{DTA}) peak at 349 ºC (Table 7). The third step, which corresponds to 17.57% loss of glycine molecule (calc. 4.86, found 4.84%) has an activation energy of 117 kJ mol^{-1}. The final residue is CuO and 0.5C as ash [(O=21.6%gly, C=8.11%gly) (calc. and found 31.78%)]. The ΔS*, ΔH* and ΔG* for these three steps are calculated (-119.3, -100.1 and -183.8 J K^{-1} mol^{-1}), (86.5, 120.2 and 114 kJ mol^{-1}) and (122.5, 153.6 and 180.7 kJ mol^{-1}), respectively.

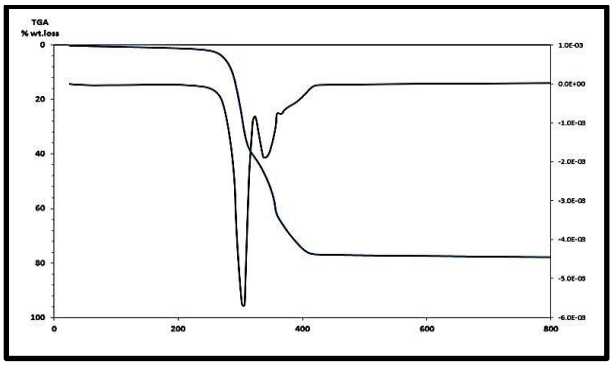

Figure 8. TG and DTG curves of $[Cu(ur)(gly)(H_2O)_2]Cl$.

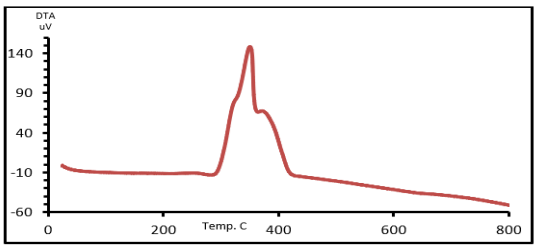

Figure 9. DTA curve of $[Cu(ur)(gly)(H_2O)_2]$ Cl.

Eclética Química Journal, vol. 43, n. 4, 2018, 25-36
ISSN: 1678-4618
DOI: 10.26850/1678-4618eqj.v43.4.2018.p25-36

Table 6. Characteristic parameters of thermal decomposition (10 °C min^{-1}) for $[Cu(ur)(gly)(H_2O)_2]Cl$.

Comp.	Step	TGA				DTA		*mass loss*
		Δm% found (calc.)	T_i/C°	T_f/C°	T_{DTG}	T_{DTA}	Heat	
$[Cu(ur)(gly)(H_2O)_2]Cl$	1	39.93 (39.95)	25	318	3.2	323	exo	-[100%H_2O+ 100%Cl +60%ur]
	2	23.43 (23.43)	318	361	334	349	exo	-[40 %ur +52.72 % gly]
	3	4.86 (4.84)	361	375	363	368	exo	-[17.57% gly]
Final residue [(CuO +0.5C) (O=21.6%gly, C=8.11%gly)]: 31.78% (31.78%)								

Table 7. Kinetic and thermodynamic parameters of the thermal decomposition of $[Cu(ur)(gly)(H_2O)_2]Cl$.

$[Cu(ur)(gly)(H_2O)_2]$ Cl	1	0.9918	3.6	$3.7x10^6$	3.2	89	-119.3	86.5	122.5
	2	0.9939	3.6	$4.1x10^7$	334	123	-100.1	120.2	153.6
	3	0.9862	4.9	$1.9x10^3$	363	117	-183.8	114	180.7

3.6. Antibacterial assay of synthesized complexes

Urea showed activity against the *Bacillus* spp. and *Escherichia coli* with inhibitory zones of 12 mm and 10 mm, respectively and glycine against the *Bacillus* with inhibitory zone of 9 mm. But no inhibition zone was observed for all the complexes against the four studied strains (*Bacillus* spp., *Escherichia coli*, *Pseudomonas aeruginosa* and *Staphylococcus aureus*) excepting the complex $[Ni(ur)(gly)(H_2O)_2]Cl$ which was active against *Escherichia coli* with inhibitory zone 5 mm. This is probably because urea denatures protein when dissolved, and for the presence of amino and carbonyl groups. However, after complexes formation there would be no activity, due to the coordination of the amino and carbonyl groups[31].

4. Conclusions

The formulae and the stoichiometry of the complexes of urea and glycine with Co(II), Ni(II) and Cu(II) metal ions are suggested based on the analytical data and TGA results. Neutral bidentate behavior of the urea coordination through the amine nitrogen and carbonyl oxygen is identified by IR spectra. Glycine behaved as an anionic bidentate ligand through the carboxylate group and the neutral amino group. The electrolytic nature of the complexes was confirmed by the molar conductance values. All the complexes have an octahedral geometry, as revealed the spectral and magnetic results. The thermal decomposition studies of $[Cu(ur)(gly)(H_2O)_2]Cl$ allowed to access the kinetic parameters for the successive steps of its decomposition. The complexes have no

Eclética Química Journal, vol. 43, n. 4, 2018, 25-36
ISSN: 1678-4618
DOI: 10.26850/1678-4618eqj.v43.4.2018.p25-36

antibacterial activities against the four strains of bacteria, except the Ni-complex, which is active against *Escherichia coli*, probably due to protein denaturation.

5. Acknowledgments

Authors are grateful to Professor Hussein Al-Maydama for his valuable assistance.

6. References

[1] Abdel-Rahman, L. H., Abu-Dief, A. M., Ismail, N. M., Ismail, M., Synthesis, characterization, and biological activity of new mixed ligand transition metal complexes of glutamine, glutaric, and glutamic acid with nitrogen-based ligands, Inorganic and Nano-Metal Chemistry 47 (3) (2017) 467-480. https://doi.org/10.1080/15533174.2015.1137057.

[2] Noyori, R., Chiral metal complexes as discriminating molecular catalysts, Science 8;248 (4960) (1990) 1194–1199. https://doi.org/10.1126/science.248.4960.1194.

[3] Li, Y. T., Yan, C. W., Zhu, Y., Guan, H. S., Synthesis and Magnetic Studies of M-Oxamidobridged Copper(II)–Manganese(II) Heterobinuclear Complexes, Synth. React. Inorg., Met-Org. Nano-Met. Chem. 34 (2005) 1165–1179. https://doi.org/10.1081/SIM-120039264.

[4] Rahaman ,S. K. H., Fun, H. K., Ghosh, B. K., A Study on Copper(II)-Schiff Base-Azide Coordination Complexes: Synthesis, X-Ray Structure and Luminescence Properties of $[Cu(L)(N_3)]X$ (L = Schiff Bases; X = ClO4, PF6), Polyhedron 24 (2005) 3091-3097. https://doi.org/10.1016/j.poly.2005.06.028.

[5] Bie, H. Y., Yu, J. H., Xu, Q. J., Li, Y.,. Cui, Y.B., Zhang, Y., Sun, Y. H., Pan, L. Y., Synthesis, Structure and Non-Linear Optical Property of a Copper(II) Thiocyanate Three-Dimensional Supramolecular Compound, Journal of .Molculare Structure 660 (2003) 107-112. https://doi.org/10.1016/j.molstruc.2003.08.011.

[6] Jan, P. A., Harold C., Helgesonb, Solubilities of The Common L-A-Amino Acids as A Function of Temperature Solution pH, Pure and Applied Chemistry 69 (5) (1997) 935-942. https://doi.org/10.1351/pac199769050935.

[7] Ivanov, A. Y., Sheina, G., Blagoi, Y. P., FTIR Spectroscopic Study of The UV-Induced Rotamerization of Glycine in The Low Temperature Matrices (Kr, Ar, Ne), Spectrochimica Acta Part A (55) (1999) 219-228. https://doi.org/10.1016/S1386-1425(98)00288-1.

[8] Doolittle, R.F., Proteins, Scientific American. 253(4) (1985) 88-91, 94-99. https://doi.org/10.1038/scientificamerican0785-72.

[9] Kandi, S., Godishala, V., Rao, P., Ramana, K. V., Biomedical Significance of Terpenes: an Insight, Biomedicine and Biotechnology 3 (1) (2015) 8-10. https://doi.org/10.12691/bb-3-1-2.

[10] Kiss, T., Sbvag , I., Gergely, A., Critical Survey of Stability Constants of Complexes of Glycine, Pure and Applied Chemistry 63 (4) (1991) 597-638. https://pubs.sciepub.com/bb/3/1/2.

[11] Jamil, Y. M., Al-Maqtari, M. A., Al-Azab, F. M., Al-Qadasy, M. K., Al-Gaadbi, A. A., Synthesis, Characterization and Comparative Thermal degradation study of Co(II), Ni(II) and Cu(II) complexes with Asparagine and Urea as mixed ligands, Eclet. Quím. J. 43 (4) (2018) 10-23. https://doi.org/10.26850/1678-4618eqj.v43.4.11-24.

[12] Siddiqi, K. S., Kureshy, R. I., Hkan, N. H., Tabassum, S., Zaidi, S. A. A., Characterization and Toxicity of Lanthanide Complexes with Nitrogen- and Sulphur-Containing Schiff Bases, Inorganic Chimica Acta 151 (1988) 95-100. https://doi.org/10.1016/S0020-1693(00)91888-7.

[13] El-Metwally, N. M., Gabr, I. M., El-Asmy, A. A., Abou-Hussen, A. A., Spectral, Magnetic, Electrical and Thermal Studies on Malonyl Bis(Thiosemicarbazide) Complexes, Transition Metal Chemistry 31 (1) (2006) 71-78. https://link.springer.com/article/10.1007/s11243-005-6347-6.

[14] Amin, R. R., Al-Subaie, A. T., El-Gamal, B. A., Mahasneh, A. M., Al-Naimi, I. S., Chemical, Synthesis, Antimicrobial Activities and Hypoglycemic Effect of Thiosemicarbazide

Derivatives, Journal of The Medical Research Institute 22 (1) (2001) 1-36. https://doi.org/10.13140/RG.2.2.35524.42885.

[15] Nakamoto, K., Infrared Spectra of Inorganic and Coordination Compounds, 2nd Edition, New York, John Wiley Interscience (1970) 166-219. https://doi.org/10.1002/ange.19650771321.

[16] Akmal, S. G., Said, M. T., El-Metwally, N., Synthesis and Spectroscopic Studies of Metal Complexes Formed in The Reaction of Metal Ions with Urea At High Temperature, Journal of The Korean Chemical Society 51 (4) (2007) 339-345. https://doi.org/10.5012/jkcs.2007.51.4.339.

[17] Refat, M. S., Mohamed, G. G., De Farias, R. F., Powell, A. K., El-Garib, M. S., Elkorashy, S. A., M. A. Hussien, M. A., Spectroscopic, Thermal and Kinetic Studies of Coordination Compounds of Zn (II), Cd (II) and Hg (II) with Norfloxacin, Journal of Thermal Analysis and Calorimetry 102 (2010) 225–232. https://doi.org/10.1007/s10973-009-0404-x.

[18] Refat, M. S., Mohamed, G. G., Ti(IV), Cr(III), Mn(II), and Ni(II) Complexes of The Norfloxacin Antibiotic Drug: Spectroscopic and Thermal Characterizations, Journal of Chemical & Engineering Data 55 (2010) 3239–3246. https://doi.org/10.1021/je100064h.

[19] Omar, B. I., Moamen, S. R., Mahmoud, S., AL-Majthoub, M. M., Chemical Studies on The Uses of Urea Complexes to Synthesize Compounds Having Electrical and Biological Applications, International Journal of Material Science 2 (3) (2012) 67-82. https://docslide.com.br/documents/tiiv-criii-mnii-and-niii-complexes-of-the-norfloxacin-antibiotic.html.

[20] Anwar, M. H., Chanmiya, S. A. Z., Mahmud, M. A. A., Synthesis and Characterization of Some Metal Complexes of Zn(II) with 1,10-Phenanthroline and Some Amino Acids: Anti-Inflammatory and Analgesic Activities of Its Complexes, International Journal of Scientific & Technology Research 2 (9) (2013) 233-237. ISSN 2277-8616. http://www.ijstr.org/final-print/sep2013/pdf.

[21] Patil, S. S., Shaikh, M. M.., Synthesis, Characterization and Antibacterial Activity of Mixed Ligand Dioxouranium Complexes of 8-Hydroxyquinoline and Some Amino Acids, Acta Poloniae Pharmaceutica - Drug Research 69 (4) (2012) 679-686. PMID: 22876610 https://europepmc.org/abstract/med/22876610.

[22] Hosny, W. M., Dioxouranium(VI) Mixed Ligand Complexes Containing 8-Hydroxyquinoline and Some Amino Acids, Synth. React. Inorg. Met. Org.Chem. 2 (1998) 1029-1052. https://doi.org/10.1080/00945719809351686.

[23] El-Asmy, A. A., Khalifa, M. E., Rakha, T. H., Hasanian, M. M., Abdallah, A. M., Mono and trinuclear complexes of oximinoacetoacetyl-pyridine-4-phenylthiosemicarbazone, Chem. Pharm. Bull. 48 (2000) 41-44. https://doi.org/10.1248/cpb.48.41.

[24] Saha, N. C., Butcer, R. J., Chaudhuri, S., Saha, N., Synthesis and spectroscopic characterisation of cobalt (III) and nickel (II) complexes with 5-methyl-3-formylpyrazole-N (4)-dibutylthiosemicarbazone (HMP z NBu 2): X-ray crystallography of [Co (MPz $NBu_2)_2$] $NO^{3\bullet}$ H_2O (I) and [Ni (HMPz $NBu_2)_2$]$(ClO_4)_2$ (II), Polyhedron 22 (3) (2003) 383-390. https://elibrary.ru/item.asp?id=1350301.

[25] El-Asmy, A. A., Mounir, M., Electrical conductivity, spectral and magnetic properties of some transition metal complexes derived from dimedone bis(4-phenylthiosemicarbazone), Transition Metal Chemistry 13 (2) (1988) 143-145. https://link.springer.com/article/10.1007/BF01087807.

[26] Amin, R. R., Elgemeie, G. E. H., The Direct Electrochemical Synthesis of Co(II), Ni(II) and Cu(II) Complexes of Some Pyridinehtione Derivatives, Synthesis and Reactivity in Inorganic and Metal-Organic Chemistry 31 (3) (2001) 431-440. https://doi.org/10.1081/SIM-100002230.

[27] El-Metwally, N. M., El-Asmy, A., Chelating Activity of Bis(Diacetylmonoxime)Thiocarbohydrazone Towards VO^{2+}, Co(II), Ni(II), Cu(II) and Pt(IV) Ions, Journal of Coordination Chemistry 59 (14) (2006) 1591-1601. https://doi.org/10.1080/00958970600572743.

[28] El-Asmy, A. A., Khalifa, M. E., Hassanian, M. M., Synthesis and Characterization of Transition Metal Complexes Containing Oxime, Amido and Thioamido Groups, Indian Journal of Chemistry 43 (A) (2004) 92-97. https://doi.org/10.1080/00958970600572743.

[29] El-Asmy, A. A., Al-Ansi, T. Y., Amin, R. R., Mounir, M. M., Spectral, Magnetic and Electrical Properties of 1-Succinyl Bis (4-Phenylthiosemicarbazide) Complexes, Polyhedron 9 (17) (1990) 2029-2034. https://doi.org/10.1016/S0277-5387(00)84032-2.

[30] El-Shekeil, A., Almaydamah, H., Al-Karbooly, A., Poly[4-Amino-2,6-Pyrimidinodithiocarbamate] and Its Cobalt, Nickel, and Copper Complexes, Journal of Inorganic and Organometallic Polymers and Materials 7 (1997) 121-133. https://doi.org/10.1023/A:1021444328744.

[31] Abdel-Rahman, L. H., Abu-Dief, A. M., Ismail, N. M., Ismael, M., Synthesis, characterization, and biological activity of new mixed ligand transition metal complexes of glutamine, glutaric, and glutamic acid with nitrogen-based ligands, Inorganic and Nano-Metal Chemistry 47 (3) (2017) 467-480. https://doi.org/10.1080/15533174.2015.1137057.

Eclética Química Journal, vol. 43, n. 4, 2018, 25-36
ISSN: 1678-4618
DOI: 10.26850/1678-4618eqj.v43.4.2018.p25-36

Eclética Química Journal

Original article
iq.unesp.br/ecletica

| Vol. 43 | n. 4 | 2018 |

Simple, fast and inexpensive method for determination of ranitidine hydrochloride based on conductometric measurements

Eduardo Henrique Bindewald[1], João Carlos da Rosa-Sobrinho[1], Márcio Fernando Bergamini[1], Luiz Humberto Marcolino-Júnior[1+]

[1] Laboratório de Sensores Eletroquímicos – LabSensE – Universidade Federal do Paraná –UFPR – Curitiba-PR, Brazil

[+] Corresponding author: Luiz Humberto Marcolino-Júnior, e-mail address: luiz1berto@ufpr.br

ARTICLE INFO

Article history:
Received: March 5, 2018
Accepted: November 2, 2018
Published: December 5, 2018

Keywords:
1. ranitidine hydrochloride
2. quality control
3. conductometric determination

ABSTRACT: This work aims the development and optimization of an alternative method for ranitidine hydrochloride (RAN-HCl) determination. The proposed method was based on conductometric titration of RAN by precipitation of AgCl solid using a solution of $AgNO_3$ as titrant. It was investigated the possibility of performing the titrations on hydroalcoholic and deionized water medium. A limit of detection of 1.0 mmol L^{-1} and 0.5 mmol L^{-1} were achieved for RAN titration in deionized water and in a 75:25 hydroalcoholic mixture, respectively. Such behavior is attributed to the dielectric constant of hydroalcoholic medium, which is lower than aqueous solution, making AgCl more insoluble and improving the resolution of the conductivity curve around the end point. Therefore, it is concluded that the conductometric titration method to determine RAN using $AgNO_3$ as titrant proved to be feasible at low drug concentrations. The statistical calculations for obtained results suggested good precision for the conductometric method. According to t-test, there were no significant differences between found values at a 95% confidence level. Moreover, obtained results showed an excellent performance of the proposed method on quality control of RAN-HCl in generic formulations without any sample pretreatment.

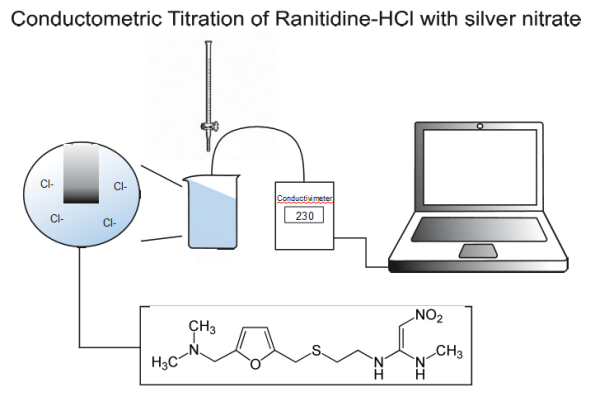

1. Introduction

In recent years, studies indicate that about 10% of the world population will suffers lesions in the gastric mucous membranes or in the duodenum[1]. The more effective treatment of this type of lesion is based on mainly administration of drugs proton pump inhibitors, as omeprazole[2]/pantoprazole[3] or anti-histamine which ranitidine hydrochloride could be highlighted[4]. Ranitidine hydrochloride (RAN-HCl - Figure 1) plays in the organism action inhibiting the secretion of gastric acid, reducing both volume and content of acid and pepsin secretion[5]. This drug is largely commercialized around the world and consequently the development of feasible, fast and sensitive methods for pharmaceutical quality control is very important.

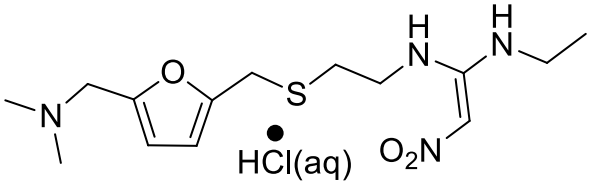

Figure 1. Molecular structure of ranitidine hydrochloride.

Eclética Química Journal, vol. 43, n. 4, 2018, 37-43
ISSN: 1678-4618
DOI: 10.26850/1678-4618eqj.v43.4.2018.p37-43

There are several procedures reported in literature for ranitidine determination based on chromatographic[6, 7], UV-Vis spectroscopy[8-10] and voltammetric methods[11-13]. British Pharmacopeia[14] describes the dosage of RAN-HCl in pharmaceutical formulations for quality control by liquid chromatography using potassium dihydrogen phosphate buffer and acetonitrile as mobile phase with UV detection. Brazilian Pharmacopeia[15] suggests direct molecular absorption spectrophotometry with detection at 314 nm as official method for determination of ranitidine hydrochloride. These cited methodologies are very reliable and exhibit sensibility, precision and accuracy adequate for concentration levels of pharmaceuticals formulations of RAN-HCl. However, these techniques demand long-time for sample preparation/treatment, use large volumes of organic solvents and/or require sophisticated and expensive instruments.

In order to overcome the drawbacks showed by other techniques, titrimetric procedures are an interesting alternative way for analysis of pharmaceutical formulations and/or biological samples, since this type of methodology is rather simple, with fast response and low-cost instrumentation. Moreover, detection of end point can be performed using an instrumental technique which is a practical approach to minimize analyst errors and leads more rapid, precise and accurate results[16].

Several "hydrochlorides" such as RAN-HCl can be found as active ingredients in commercialized pharmaceutical formulations. In general, hydrochlorides are more water-soluble and provide better absorption by human body[17]. Some methodologies have been described for determination of these compounds, based on indirect quantification of drug based on chloride ions released from salt dissolution[18-21]. Caetano *et al.*[18] reported a low-cost conductometric method for determination of verapamil hydrochloride in pharmaceutical formulations based on chloride ions released from verapamil hydrochloride which were titrated with an aqueous solution of silver nitrate. Similar approach was adopted by Noronha *et al.*[19] who described potentiometric and conductometric titration of diltiazem hydrochloride (DTZ) determination based on the chemical reaction between chloride ions coming from diltiazem hydrochloride molecule and Ag(I) ions, yielding the precipitate AgCl solid. The limit of applicability of the conductometric method based on precipitation titration is defined by solubility of solid yielded AgCl (Kps ~1.8 x 10^{-10}). The solubility product constant can be affected by alteration in the dielectric constant of the solvent (ε) allowing to use lower concentration level of reagents. A decrease in the Kps could be obtained simply using of hydroalcoholic medium which presents a minor value of dielectric constant when compared to aqueous solution. This effect plays an important role in the precipitation titration procedure allowing the use of lower quantity of reagents.

Based on above-cited information, the present work describes a practical and accurate methodology for RAN hydrochloride determination based on conductometric titration of chloride ions using by $AgNO_3$ as titrant in hydroalcoholic medium.

2. Materials and methods

2.1. Instruments, reagents and chemicals

A system comprising by Conductometer Oakton® COM 500 and a classic burette of 25.0 mL associated with a magnetic stirrer were used for all conductometric measurements. The solutions were prepared with deionized water obtained from Milli-Q system or ethanol (Carlo Erba, 99.9%). Other used reagents were silver nitrate and sodium chloride (Merck, > 99% content) and ranitidine hydrochloride (Aldrich, > 95% content).

Silver nitrate solutions were used in the titration of the same concentration of ranitidine solutions ranging from 0.10 to 1.0 x 10^{-3} mol L^{-1}. The same were standardized using anhydrous sodium chloride as primary standard. For comparative method, a spectrophotometer Hewlett Packard, model 8452A equipped with 1.0 cm light path quartz cuvette. Acid-base titrations were performed using a 780 pHmeter Metrohm equipped with combined glass electrode associated a classic burette of 25.0 mL and magnetic stirrer.

2.2. Samples and standard solutions

Pharmaceutical samples in tablet form containing ranitidine hydrochloride (RAN-HCl) were purchased in local drugstore. For each sample, twenty tablets were crushed using mortar and pistil and 50.0 mL of a stock solution with theoretical concentration of 1.0 mmol L^{-1} was

Eclética Química Journal, vol. 43, n. 4, 2018, 37-43
ISSN: 1678-4618
DOI: 10.26850/1678-4618eqj.v43.4.2018.p37-43

prepared using deionized water or hydroalcoholic solution in different proportions of solvent.

2.3. Conductometric titration

Aliquots of 10.0 mL or 5.0 mL (reference solutions or sample) were transferred to beakers and titrated with solutions of $AgNO_3$ at the same concentration of the analyte (between 5.0 x 10^{-4} to 0.1 mol L^{-1}) with additions of 0.5 mL or 1.0 mL. Conductance values were recorded 10 seconds after the titrant addition. Before plotting titration graphs, conductance values were corrected according to volume of titrant added (Equation 1), all titrations were conducted in temperature controlled at 20 ºC.

$$L_{corr} = L_{exp} * \left({(V_{ini} + V_{add})}/{V_{ini}} \right) \quad (1)$$

where: L_{corr} = corrected conductance, L_{exp} = experimental conductance, and V_{ini}, V_{add} the initial volume and added volume, respectively.

From graph of corrected conductance *vs.* volume of $AgNO_3$ solution, the end point was obtained by the intersection of the straight-line segments, and thus determining the concentration of RAN-HCl.

2.4. Acid-Base titration (pH curves)

A standard solution of RAN-HCl, 0.10 mol L^{-1} was titrated with NaOH at the same concentration, previously standardized by sodium biphthalate. Based on the pH *vs.* NaOH volume curve was possible to estimate the pKa of RAN-HCl. The pKa value was estimated using the pH obtained at ½ volume of the end point.

2.5. Comparative method

Comparative method used is described on Brazilian Pharmacopeia[13] based on UV-Vis spectroscopy. A portion equivalent to one tablet was dissolved in water and after diluting to concentration around to 0.00125% (w/v). Standard solution was prepared at same concentration and the absorbance measurements of samples and standards solution were carry out at 314 nm using a quartz cuvette.

3. Results and discussion

3.1 Preliminary studies

Firstly, the potentiality of conductometric titration for proposed determination was investigated in order to show that indirect quantification of RAN-HCl can be realized based on precipitation reaction between Cl^- and Ag^+ ions leading to formation of AgCl. An aliquot of 10.0 mL of 0.10 mol L^{-1} RAN-HCl standard solution was prepared in deionized water and it was titrated with a standardized solution of $AgNO_3$ at the same concentration (Figure 2). Typical conductometric curve for titration of RAN-HCl with silver nitrate shows two linear segments with significant difference in the slope. Before the endpoint, no significant variation of conductance values was observed which is attributed to consume of chloride ions by precipitation of AgCl (solubility, 1.1 x 10^{-5} mol L^{-1}) concomitantly with reposition of nitrate ions from $AgNO_3$. Slight variation in conductance observed in this segment can be attributed to exchange of ions with very similar ionic mobility (Cl^- 76.3 S cm^2 mol^{-1} and NO_3^- 71.5 S cm^2 mol^{-1}). After the endpoint, a marked increase of conductance values was observed due to excess of silver and nitrate ions in solution. The endpoint was determined by intersection of segment #1 and #2 and RAN-HCl concentration was estimated based on 1:1 stoichiometric relationship.

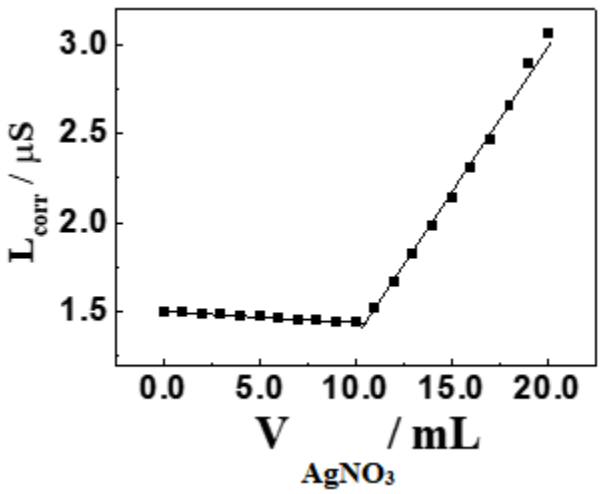

Figure 2. Representative conductometric curve obtained for titration of 10.0 mL of 0.10 mol L^{-1} RAN-HCl standard aqueous solution with a standardized solution of $AgNO_3$ 0.10 mol L^{-1}.

Eclética Química Journal, vol. 43, n. 4, 2018, 37-43
ISSN: 1678-4618
DOI: 10.26850/1678-4618eqj.v43.4.2018.p37-43

The proposed procedure is based on determination of chloride ions released from RAN-HCl after its dissolution (RAN-HCl(s) + H_2O → RAN(aq) + H_3O^+(aq) + Cl^-(aq)). Potentiometric titration of RAN-HCl with NaOH standard solution was performed in order to verify adequate reactions that occur during the conductometric titration. In Figure 3A is possible to observe a curve with similar shape to obtained titration for systems composed by weak acid titrated with strong base (endpoint is observed at pH > 7.0). Additionally, from titration curve the pKa value for reaction RAN-H^+ + H_2O ⇆ RAN + H_3O^+ was estimated as 8.05 ± 0.10 (n = 3). Thus, based on these results we believe that reactions involved in the proposed procedure could be better attributed to: RAN-HCl(s) → RAN-H^+(aq) + Cl^-(aq) (dissolution step) and Ag^+(aq) + Cl^-(aq) →AgCl(s) (titration step).

UV-vis spectrophotometric measurements were performed at different pH values in order to confirm the protonation of ranitidine molecule. Figure 3B shows UV-vis spectra where an increase in the absorption intensity at 310 nm with the increase of pH values can be observed. This behavior is attributed to protonation of RAN molecule which is majority form at pH values at least 2.0 units lower than pKa. These studies confirm that the conductometric titration was performed with RAN molecules in the protonated form.

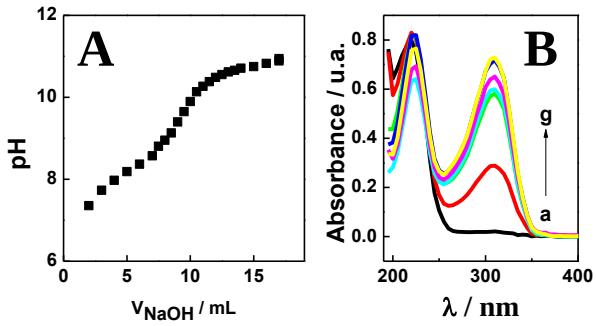

Figure 3. A) pH curve obtained for titration of RAN-HCl using NaOH standardized solution; B) Absorption spectrum in the UV-Vis region for RAN-HCl in pH values: 1.0 (a), 2.0 (b), 2.5 (c), 3.0 (d), 4.0 (e), 5.0 (f) and 6.0 (g).

3.2. Optimization of the titration method

Several investigations were realized in order to optimize the proposed methodology. For this, all solutions were prepared with deionized water to obtain a lower background signal. Firstly, the effect of solution concentration (titrant and titrated) has been evaluated by performing of three successive titrations using concentrations in range between 0.50 and 10.0 mmol L^{-1}. Table 1 presents results of recovery studies.

Table 1. Titrations realized with deionized water.

Concentration of ranitidine added / mmol L^{-1}	Concentration of ranitidine found / mmol L^{-1}	Recovery
10	9.9	99%
1.0	0.92	92%
0.50	-	ND

ND: Not detected

Adequate recoveries values were obtained using solutions with concentration of 10.0 mmol L^{-1} indicating a well-defined shape of titration curve. When concentrations of 1.0 mmol L^{-1} were used, a significant decrease in recoveries values were found suggesting a poor profile of the conductometric titration curve. Concentration lower than 1.0 mmol L^{-1} did not provide a variation in the conductance of solution which did not allow found an end point from titration curve. Thus, the best set of results using aqueous solutions were found only for concentrations higher than 1.0 mmol L^{-1}.

In order to achieve detections below the limit imposed by use of aqueous solution, we decided to try to alter the solubility of solid formed (AgCl) during titration process by using of another solvent mixed on aqueous solutions. The adopted strategy was based on variation of dielectric constant (ε) of solution. The dielectric constant of a solvent could be related with its polarity and ability for solvation of ions. When a dielectric constant of solvent is higher it means that this solvent is more polar, and it is more efficient to solvate the ions. As consequence of this, an increase in solubility of ionic solid could be observed for solvent with high

Eclética Química Journal, vol. 43, n. 4, 2018, 37-43
ISSN: 1678-4618
DOI: 10.26850/1678-4618eqj.v43.4.2018.p37-43

dielectric constant. The dielectric constant of water is 78.3 (25 °C) and it is higher than ethanol (24); so, a higher solubility of AgCl solid in water is verified when compared with ethanol. In this way, the use of hydroalcoholic solutions promotes a decrease in the solubility of silver chloride and allows to use of more dilute solutions in the conductometric titration. Titrations employing hydroalcoholic solutions in the range of 0 to 75% (v/v) of ethanol were performed using 1.0 mmol L^{-1} of RAN-HCl and $AgNO_3$ in order to investigate the effect of mix of solvents (Figure 4).

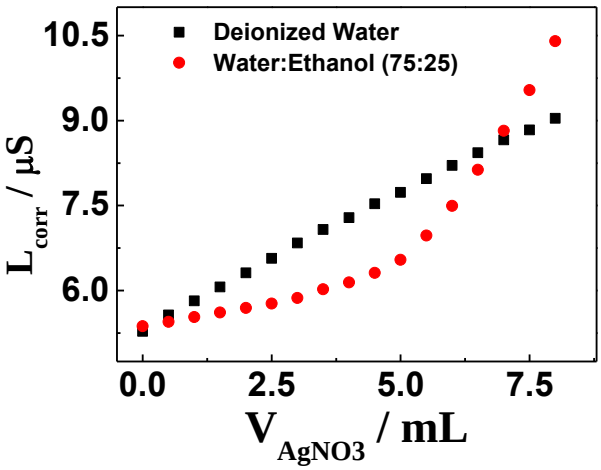

Fig. 4 Titrations conductometric curves obtained using different solvents composition.

By using of hydroalcoholic solutions, recoveries values close to 100% were obtained for all titrations, indicating that presence of ethanol as solvent results in an improvement in the determination. Amounts of ethanol higher than 50% did not yield significant differences between the segments of titration curve which can be related with decrease in the solubility of reagents. For larger amounts of alcohol (25:75 water:ethanol) there was a decrease in sensitivity caused by a poor solubility of $AgNO_3$. Using a composition of 75:25 water:ethanol, it was possible to determine the concentration of RAN-HCl employing concentration of 0.5 mmol L^{-1} for reagent which was not achieved performing the titration in water. Such behavior was attributed to the lower dielectric constant inherent to the solution which resulted in a lower background signal enabling the identification of titration equivalence point with good reliability.

3.3. Determination of RAN-HCl in pharmaceutical samples

After the optimization of experimental conditions, the proposed method was applied for determination of RAN-HCl in triplicate for three different samples of pharmaceutical formulations (Table 2). Results obtained using the conductometric titration were compared with those provided using the spectrophotometric method recommended by the Brazilian Pharmacopoeia and the values given on the pharmaceutical formulations labels.

Table 2. Results of determination of RAN-HCl in pharmaceutical formulations.

	Sample	Labeled values / mg	Proposed Method / mg	Reference Method / mg	RSD*
1	Generic	300	305 ± 9	298.4 ± 0.7	2.1%
2	Generic	150	158.7 ± 0.3	165 ± 6	3.5%
3	Generic	150	161.1 ± 0.2	163 ± 5	1.0%

*RSD: relative standard deviation (Proposed *vs.* Reference Method)

Statistical test suggested good accuracy for the conductometric method in comparison with official methodology, indicating that the excipients used to manufacture the tablets of ranitidine formulations did not exhibit interference in the determination of the drug[18-20]. According to the t-test, there were no significant differences between the values found at the 95% confidence level. Moreover, results obtained showed an excellent performance of proposed method to quality control of RAN-HCl in generic formulations without any sample pretreatment.

Eclética Química Journal, vol. 43, n. 4, 2018, 37-43
ISSN: 1678-4618
DOI: 10.26850/1678-4618eqj.v43.4.2018.p37-43

4. Conclusions

This study demonstrated that conductometric titration is a very powerful methodology for determination of ranitidine hydrochloride, being a simple, fast and inexpensive alternative route to perform quality control of these species, especially in small laboratories. The use of hydroalcoholic solutions allowed a decrease in the detection limit of the technique. It was possible to perform quality control of RAN-HCl in the order of 0.5 mmol L^{-1} with significant reducing costs. Pharmaceutical samples without any pretreatment were analyzed using proposed titration and values with excellent agreement with an official method were found.

5. Acknowledgments

We gratefully acknowledge financial support from Fundação Araucária, CAPES, and CNPq.

6. References

[1] Saul, C., Teixeira, C. R., Pereira-Lima, J. C., Torresini, R. J. S., Redução da prevalência de úlcera duodenal: Um estudo brasileiro (análise retrospectiva na última década: 1996-2005), Arquivos de Gastroenterologia 44 (4) (2007) 320-324. https://doi.org/10.1590/S0004-28032007000400008.

[2] Jorge, S. M. A., Pontinha, A. D. R., Oliveira-Brett, A. M., Electrochemical Redox Behavior of Omeprazole Using a Glassy Carbon Electrode, Electroanalysis 22 (6) (2010) 625-631. https://doi.org/10.1002/elan.200900377.

[3] Huber, R., Hartmann, M., Bliesath, H., Lühmann, R., Steinijans, V. W., Zech, K. (i), Pharmacokinetics of pantoprazole in man, International Journal of Clinical Pharmacology and Therapeutics, 34 (1 Suppl.) (1996), S7-16. Retrieved from http://europepmc.org/abstract/med/8793599.

[4] De Armas, H. N., Peeters, O. M., Blaton, N., Van Gyseghem, E., Martens, J., Van Haele, G., Van Den Mooter, G., Solid state characterization and crystal structure from x-ray powder diffraction of two polymorphic forms of ranitidine base, Journal of Pharmaceutical Sciences, 98 (1) (2009) 146–158. https://doi.org/10.1002/jps.21395.

[5] Madsen, J. L., Graff, J., Effects of the H_2-receptor antagonist ranitidine on gastric motor function after a liquid meal in healthy humans, Scandinavian Journal of Clinical and Laboratory Investigation 68 (8) (2008) 681–684. https://doi.org/10.1080/00365510802047685.

[6] Arayne, M. S., Sultana, N., Zuberi, M. H., Siddiqui, F. A., Simultaneous determination of metformin, cimetidine, famotidine, and ranitidine in human serum and dosage formulations using HPLC with UV detection, Journal of Chromatographic Science 48 (9) (2010) 721-725. https://doi.org/10.1093/chromsci/48.9.721.

[7] Tatar Ulu, S., Tuncel, M., A sensitive and rapid determination of ranitidine in human plasma by HPLC with fluorescence detection and its application for a pharmacokinetic study, Journal of Chromatographic Science 50 (4) (2012) 301-306. https://doi.org/10.1093/chromsci/bms003.

[8] Cholerton, T. J., Hunt, J. H., Klinkert, G., Martin-Smith, M., Spectroscopic Studies on Ranitidine - its Structure and the Influence of Temperature and pH, Journal of the Chemical Society, Perkin Transactions 2 4 (11) (1984) 1761-1766. https://doi.org/10.1039/P29840001761.

[9] Elgailani, I. E. H., Mohammed A. A., Spectrophotometric Determination of Some Antiulcerative Drugs in Pharmaceutical Dosages, Journal of Analytical Chemistry 73 (7) (2018) 679-684. https://doi.org/10.1134/S1061934818070079.

[10] de Araújo, W. R., Paixão, T. R. L. C., Amperometric detection of ranitidine using glassy carbon modified with ruthenium oxide hexacyanoferrate adapted in a flow injection system, Electroanalysis 23 (11) (2011) 2549-2554. https://doi.org/10.1002/elan.201100102.

[11] Xi, X., Ming, L., Electrochemical determination of ranitidine hydrochloride in pharmaceutical formulations and biological fluids at graphene modified electrode, Asian Journal of Chemistry 25 (10) (2013) 5315-5318. https://doi.org/10.14233/ajchem.2013.14172.

[12] Pınar, P. Talay, Y. Yardım, Z. Şentürk, Electrochemical oxidation of ranitidine at poly (dopamine) modified carbon paste electrode: Its voltammetric determination in pharmaceutical and

biological samples based on the enhancement effect of anionic surfactant, Sensors and Actuators B: Chemical 273 (2018) 1463-1473. https://doi.org/10.1016/j.snb.2018.07.068.

[13] Moldovan, Z., Aboul-Enein, H. Y., Spectrophotometric method for ranitidine determination in drugs using Rhodamine B, Journal of the Chilean Chemical Society 57 (4) (2012) 1422–1427. https://doi.org/10.4067/S0717-97072012000400018.

[14] British Pharmacopoeia Commission, Great Britain, Medicines Commission, and General Medical Council (Great Britain). British Pharmacopoeia. Vol II. Ranitidine Hydrochhoride 209 (2000) 5168-5173.

[15] Farmacopéia Brasileira, Vol. II, 5th ed., Agência Nacional de Vigilância Sanitária, Brasília, Brazil 2010, p. 225.

[16] Weber, C., Heuser, M., Mertens, G., Stanjek, H., Determination of clay mineral aspect ratios from conductometric titrations, Clay Minerals 49 (1) (2014) 17-26. https://doi.org/10.1180/claymin.2014.049.1.02.

[17] Allen, L. V., Remington: An Introduction to Pharmacy, Pharmaceutical Press, Retrieved from http://books.google.ca/books?id=J_6H4HfqdJkC.

[18] Caetano, F. R., Gevaerd, A., Bergamini, M. F., Marcolino-Junior, L. H., A Fast and Simple Conductometric Method for Verapamil Hydrochloride Determination in Pharmaceutical Formulations, Current Pharmaceutical Analysis 7 (4) (2011) 275-279. https://doi.org/10.2174/157341211797458041.

[19] de Noronha, B. V., Papi, M. A. P., Bergamini, M. F., Marcolino-Junior, L. H., A Simple and Precise Determination of Diltiazem Hydrochloride by Simultaneous Conductometric and Potentiometric Detection, Current Pharmaceutical Analysis 10 (3) (2014) 203-207. https://doi.org/10.2174/1573412910666140403000201.

[20] Sartori, E. R., Suarez, W. T., Fatibello-Filho, O., Determinação condutométrica de cloridrato de metformina em formulações farmacêuticas empregando nitrato de prata como titulante, Química Nova 32 (7) (2009) 1947-1950. Retrieved from http://www.scielo.br/scielo.php?script=sci_arttext&pid=S0100-40422009000700043&nrm=iso.

[21] Diamandis, E. P., Christopoulos, T. K., Potentiometric titration of pharmaceutical compounds in formulations with sodium tetraphenylborate, Analytica Chimica Acta 152 (C) (1983) 281-284. https://doi.org/10.1016/S0003-2670(00)84919-3.

Eclética Química Journal

Original article
iq.unesp.br/ecletica

| Vol. 43 | n. 4 | 2018 |

Dark breather using symmetric Morse, solvent and external potentials for DNA breathing

Hernán Oscar Cortez Gutierrez[1+], Milton Milciades Cortez Gutierrez[2], Girady Iara Cortez Fuentes Rivera[3], Liv Jois Cortez Fuentes Rivera[4], Deolinda Fuentes Rivera Vallejo[3]

[1] Universidad Nacional del Callao, Facultad de Ciencias de la Salud, 306 Juan Pablo II Av, Callao, Bellavista, 07001, Peru
[2] Universidad Nacional de Trujillo, 555 Jr. Salaverry Urb. Mansiche, Peru
[3] Universidad Inca Garcilaso de la Vega, 890 San Felipe Av., Jesús María, Lima, Peru
[4] Universidad Privada San Juan Bautista, José Antonio Lavalle St., Distrito de Chorrillos, 15067, Peru

[+] Corresponding author: Hernan Oscar Cortez Gutierrez, phone: +51 964353795, e-mail address: hcortez@unac.pe

ARTICLE INFO

Article history:
Received: April 29, 2018
Accepted: October 13, 2018
Published: December 5, 2018

Keywords:
1. Mobile dark breather
2. Center of energy
3. quantum thermodynamics
4. DNA breathing

ABSTRACT: We analyze the dynamics and the quantum thermodynamics of DNA in Symmetric-Peyrard-Bishop-Dauxois model (S-PBD) with solvent and external potentials and describe the transient conformational fluctuations using dark breather and the ground state wave function of the associate Schrodinger differential equation. We used the S-PBD, the Floquet theory, quantum thermodynamic and finite difference methods. We show that for lower coupling dark breather is present. We estimate the fluctuations or breathing of DNA. For the S-PBD model we have the stability of dark breather for k<0.004 and mobile breathers with coupling k=0.004. The fluctuations of the dark breather in the S-PBD model is approximately zero with the quantum thermodynamics. The viscous and external potential effect is direct proportional to hydrogen bond stretching.

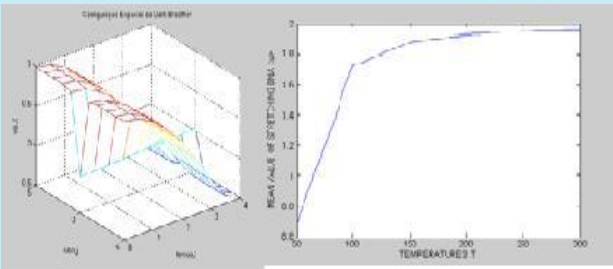

1. Introduction

The deoxyribonucleic acid DNA is a thread-like chain of nucleotides carrying the genetic information of all organisms. The coding sequences for genes and regulatory information are located in DNA and is marginally stable and undergoes a "melting phase transition". There are many experimental ways to study the fluctuations or breathing of DNA: hydrogen exchange, formaldehyde probing, protein-nucleic acid interactions, DNA replication, DNA base analogue spectroscopy, single molecule DNA-protein interactions, two-dimensional fluorescence spectroscopy[1]. The interaction between the viscous potential and external forces prevent DNA to unzip perfectly but allows DNA to split at a certain distance from its original position[2]. S. Flach gives the theory of the "discrete breathers" and applications[3].

R. S. Mackay investigates the Peyrard Bishop model for the study of nonlinear excitations travelling along the DNA chains[4]. J. Cuevas has results about breathing of DNA using the spatially localized oscillations or 'discrete breathers'[5]. The mobility and breathing of DNA depends on the harmonic bifurcation[6]. The strong dependence on sequence, temperature and salt concentration for the breathing dynamics of DNA found here points

CC BY

Eclética Química Journal, vol. 43, n. 4, 2018, 44-49
ISSN: 1678-4618
DOI: 10.26850/1678-4618eqj.v43.4.2018.p44-49

at a good potential for applications and the effect of the viscous and external forces[2, 7].

First, the PBD model is introduced. It is then followed by the dynamical and the thermodynamic formulations. We show that mobile breather can lead to the observed breathing, but the amplitude of the breather is determinant for the transient conformational fluctuations of DNA. The results obtained in our simulation verify the existence of dark breather with the conditions describes by R.S. Mackay. The symmetric potential does not give a solution for the transition of the DNA. For that reason, it is necessary to investigate the effect of the solvent and external potentials. The calculation of hydrogen bond stretching using transfer integral operator and difference finite methods are presented.

2. Materials and methods

2.1 Symmetric Morse Potential in the PBD model

The biomechanics of DNA is represented by two degree of freedom X_n and Y_n which correspond to the displacement of the base pair from their equilibrium position along the direction of the hydrogen bonds connecting the two-base pair of nucleotides.

The studies of the Symmetric Peyrard-Bishop-Dauxois (S-PBD) models that included the modified Morse potential was done by adding the absolute value:

$$V(u) = \frac{1}{2}\left[\exp(-|u|) - 1\right]^2 \qquad (1)$$

where V = symmetric Morse Potential.

The profile of symmetric Morse potential can be seen in Figure 1.

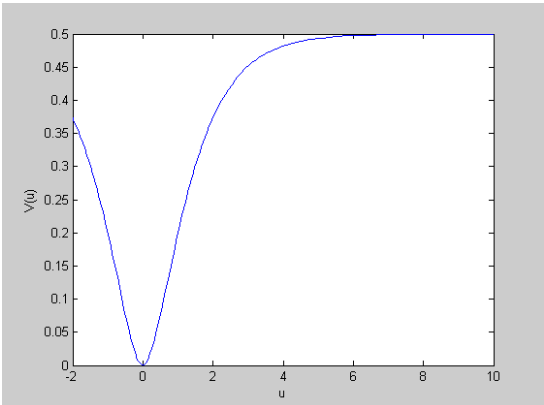

Figure 1. The symmetric Morse potential**.**

$$H = \sum_{n=1}^{N} \frac{m}{2} \dot{u}_n^2 + \sum_{n=1}^{N} \frac{K}{2}(u_n - u_{n-1})^2 + \sum_{n=1}^{N} V_n(u_n) \qquad (2)$$

where N = number of the pairs of bases; K = *velocity* = *u* coupling constant; and u_n = stretching of the hydrogen bonds = $(X_n - Y_n)/\sqrt{2}$.

2.2 Dynamics of S-PBD

The associated equations for Equation 4 are the system equations (n=1, 2... N):

$$\ddot{u}_n + sign(u_n)\left[e^{-2/u_n/} - e^{-/u_n/}\right] + K(2u_n - u_{n-1} - u_{n+1}) = 0 \qquad (3)$$

Using the approximation for the oscillator n and $T=2\pi/w_b$

$$u_n = z_n^0 + \sum_{k=1}^{k_m} 2z_n^k \cos(k\omega_b t) \qquad (4)$$

and substituting in Eq. 3 one has:

$$k^2\omega_b^2 z^2{}_n + V_n'^k + K(2z^k{}_n - z^k{}_{n-1} - z^k{}_{n+1}) = 0 \qquad (5)$$

which depends on the parameter K, and $V'_n{}^k$ is the kth Fourier coefficient for the periodic Function $V'(u_n(t))$.

Remark 1. <u>One site dark breather</u>

The dark breather solution is obtained in conditions (t=0) where all the oscillators are at rest, but equally shifted from their equilibrium position, while the central one is at the rest. The codification for one site dark breather is 1,1,…1,0,1,…,1,1.

In Fig. 2 the dark breather is depicted. This figure shows the numerical solution of equation (5). The second derivative of the symmetric Morse potential is given by:

$$V'' = \left[2e^{-2/u_n/} - e^{-/u_n/}\right].$$

Eclética Química Journal, vol. 43, n. 4, 2018, 44-49
ISSN: 1678-4618
DOI: 10.26850/1678-4618eqj.v43.4.2018.p44-49

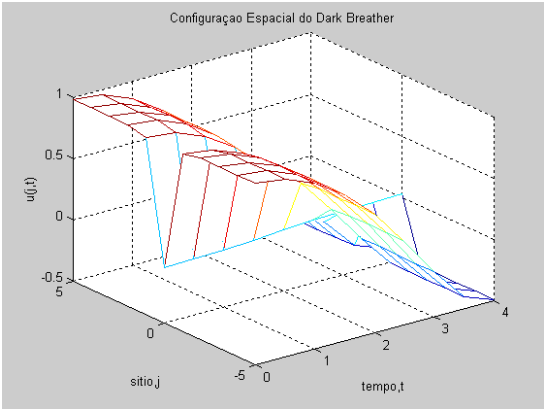

Figure 2. Spatial dark breather configuration of the symmetric Morse potential.

The dynamics of the DNA is a set of coupled oscillators, and the vibrational motion is equivalent to equation (3) which depends of the Symmetric Morse potential and constant *K* of coupling.

The amplitude of the breather is determinant for the transient conformational fluctuations of DNA. In our case the Figure 2 give a small amplitude.

2.2.1 Existence of Harmonic bifurcation

We analyze the stability of the breather solution. Let us introduce a function $\tilde{u}_n(t) = u_n(t) + \varepsilon_n(t)$, where $u_n(t)$ is the periodic breather solution shown in Figure 2. The term $\varepsilon_n(t)$ is a perturbation: $\tilde{u}_n(t)$ must satisfy the system (3) and expanding around $u_n(t)$ to first order (linearization), we obtain the following system of equations for $\varepsilon_n(t)$

$$\ddot{\varepsilon}_n + \left(V''(u_n(t))\right)\varepsilon_n + K(2\varepsilon_n - \varepsilon_{n-1} - \varepsilon_{n+1}) = 0 \quad (6)$$

We can associate a monodrama my matrix for this equation with Fouquet multipliers[5].

The solution is stable if the modules of Fouquet multipliers are one. The especial instability ("harmonic bifurcation") in our case happens when a pair of Fouquet multipliers merges at $\lambda = 1$ and splits off circle onto the positive real axis in Fig. 3.

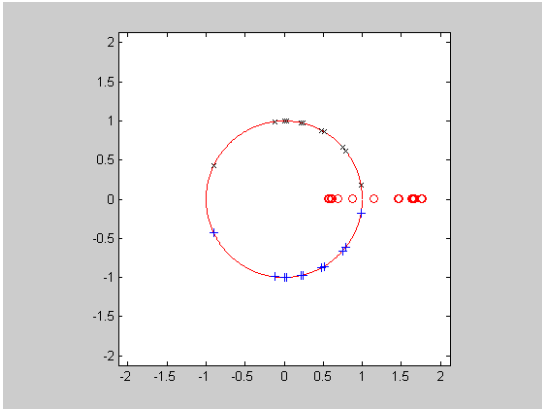

Figure 3. The instability "harmonic bifurcation" with the evolution of the Fouquet multipliers. Case SPBD model with the parameters: *K*=0.004, w_b=0.8 for the dark breather.

2.2.2 Existence of Mobile breather

For the coupling *K*=0.004 and w_b =0.8 there is a harmonic bifurcation. In this case we can construct a dark breather mobile. Once the system of equations (3) is worked out by Runge Kutta method for the Cauchy problem with the equations (3). We can use the Figure 2 for the initial conditions of the position and average speed of each position "*n*" respect to the harmonic oscillation corresponding to the DNA.

The center of energy of the breather mobile is given by[5]

$$X_E = \sum_{n=1}^{N} n H_n^d \ / H \quad (7)$$

where the density energy has the form

$$H_n^d = \frac{1}{2}\dot{u}_n^2 + \frac{K}{4}(u_n - u_{n-1})^2 + \frac{K}{4}(u_{n+1} - u_n)^2 + V_n(\sqrt{2}u_n) \quad (8)$$

It is very important the initial velocity of the BM for the displacement a long of sites of DNA and can be produced of DNA breathing.

This parameter initial velocity *v(0)* is transcendental for DNA breathing.

Remark 2. <u>Initial velocity and the perturbation velocity</u>

We can use the profiles of the stationary dark breather obtained from equations (3). The velocity is a vector which the components are given by

$$v_n(0) = (u_{n+1}(0) - u_{n-1}(0))/2 \quad (9)$$

Eclética Química Journal, vol. 43, n. 4, 2018, 44-49
ISSN: 1678-4618
DOI: 10.26850/1678-4618eqj.v43.4.2018.p44-49

We can define a perturbation velocity in terms of the parameter λ. The components of this vector perturbation *V* are given by

$$V_n(0) = \lambda(v_n(0)/v) \tag{10}$$

Where *v* is the norm of the vector of the components $v_n(0)$.

Remark 3. The Cauchy problem is given by

$$\ddot{u}_n + V'(u_n) + K(2u_n - u_{n-1} - u_{n+1}) = 0 \tag{11}$$

Initial conditions: $u_n(0)$ = profiles of the solutions of the Figure 2. The velocities are given by the expression (10) with λ = 0.1. We can obtain the solutions of the equations using initial condition with the software Fortran (for a review, see ref. 9).

2.3 Quantum Thermodynamics of S-PBD

The evaluation of the partition of equation (2) using the transfer integral operator method in the thermodynamic limit reduces to solving the pseudo-Schrodinger equation (12):

$$\{-1/(2\beta^2 K)d^2/du_n^2 + U(u_n,\beta)\}\psi(u_n) = \varepsilon\psi(u_n) \tag{12}$$

$$U(u_n,\beta) = V(\sqrt{2}u_n) + (1/2\beta)\ln(\beta K/2\pi) \tag{13}$$

$$\beta = 1/(K_B T) \tag{14}$$

We use the symmetric Morse potential. The fluctuations or breathing of DNA can be performed numerically using the finite difference methods. Firstly, we obtain the ground state wave function of equation (12). For estimate the mean value of the fluctuations we use the formula:

$$<u> = \int_{-\infty}^{+\infty} \psi^2{}_0 u du \tag{15}$$

The ground state wave function for the symmetric Morse potential is symmetric in consequence the mean value of the fluctuations is approximately zero (for a review, see ref. 12).

In Figure 4 is depicted the example of the ground state wave function for the symmetric Morse potential.

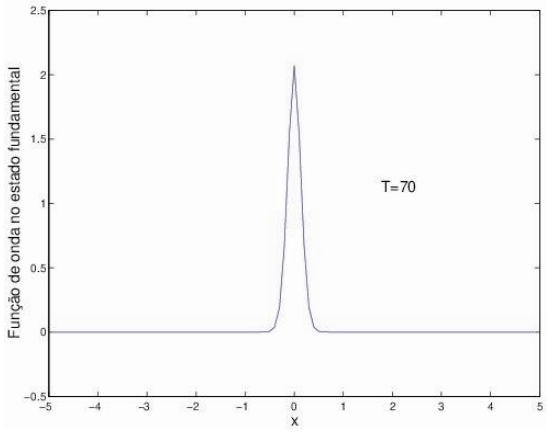

Figure 4. Ground state wave function for the symmetric Morse potential with the control parameter Temperature=70 °K.

2.3.1 Quantum Thermodynamics of S-PBD with solvent and external potentials

We can consider the new potential for the equation (13):

$$U(u_n) = V(\sqrt{2}u_n) + Vsolvent(u_n) + V_0 \exp(-0.1u_n^2) + (1/2\beta)\ln(\beta K/2\pi) \tag{16}$$

The solvent potential is given by: $V_{solvent}$ = 0.04*ν*tanh (u_n/5 -1). In Figure 5, it is depicted the example of the solvent potential.

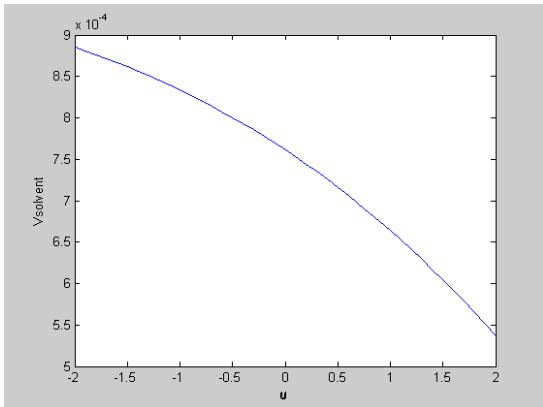

Figure 5. The solvent potential with the control parameter ν=0.025.

For the symmetric Morse potential in the S-PBD Model we can get many values of the melting temperatures. For example, for T =270 K and the control parameter ν = 0.001, V_0 = 0.005 the mean value of the fluctuations <*u*> = 1.9586 Å. The hydrogen bond stretching as a function of

Eclética Química Journal, vol. 43, n. 4, 2018, 44-49
ISSN: 1678-4618
DOI: 10.26850/1678-4618eqj.v43.4.2018.p44-49

temperature gives a melting temperature depicted in Figure 6.

Bustamante[13] has the interplay between the "DNA breathing" with the viscosity coefficient of the medium.

a)

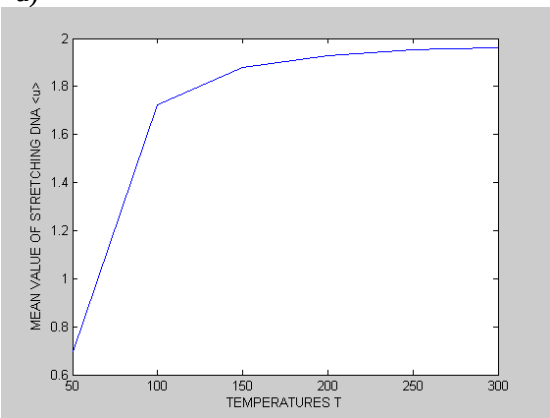

b)

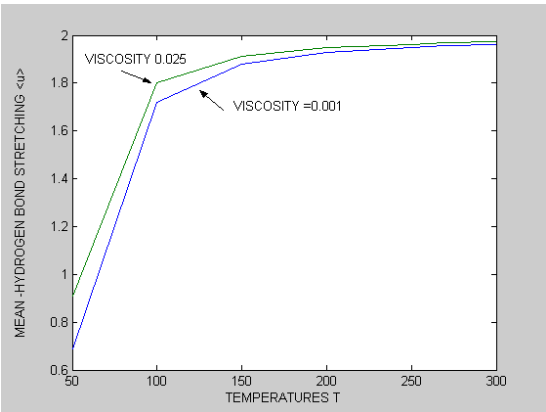

Figure 6. The hydrogen bond stretching as a function of temperature for external.

Potential $V = V_0 \exp(-0.1\, u^2)$, V_0 =0.005 and solvent potential with the viscosity control parameter *v: a*) v=0.001 and b) v=0.025.

3. Results and discussion

The solutions of the dynamical equations (5) give the dark breather mobile. We have the mobile breather using the center of energy for the initial velocity of 0.1. This method is based on the literature[6, 8].

We have obtained harmonic bifurcation using the symmetric Morse potential with the parameter *K*=0.004.

We have obtained the Eigen functions of the pseudo-Schrodinger equation (12) to demonstrate that the mean value breathing of DNA is zero. The analysis is based on the reference[12].

For the symmetric Morse potential in the S-PBD Model, we can get the melting temperature for T = 270 K, control viscosity parameter v = 0.001 and the constant of the external potential V_0 = 0.005. For these values the mean value of the fluctuations <*u*> is 1.9586 Å. In this case, we can get the DNA breathing with the variations of temperatures (Figure 6a).

Figure 6b indicates that mean value of stretching <*u*> is direct proportional to the coefficient of viscosity. The increase of the viscosity will increase the hydrogen bond stretching. The viscous and external potential effect is direct proportional to hydrogen bond stretching. For V_0 = 0.5 the mean value of hydrogen bond is <*u*>= 3.82 with the temperature T = 270 K and viscosity v = 0.025.

The Figure 6 shows that for T > 150 K the viscous force is not important for the DNA breathing. This result is similar to that obtained in the literature[2].

4. Conclusions

The stability of dark breathers using of the symmetric Morse potential have been obtained with the Floquet's theory. It is very important to emphasize that dark breathers at low coupling are shown to be stable in the PBD model with k<0.004. For k=0.004 we have harmonic bifurcation and the mobile dark breather. In this case and using numerical simulations we can demonstrate that the mean value of the hydrogen bond stretching is zero.

For the symmetric potentials we have significant fluctuations in the analysis of the breathing DNA with solvent and external potentials. The external potential is more important than the viscous force for the estimated melting temperature and the mean value of the hydrogen bond stretching.

5. Acknowledgments

The authors would like to acknowledge the Universidad Nacional del Callao-Facultad Ciencias de la Salud for the technological support. We would also like to thank Walter Julio Cortez Morales and Olga Estrada for economical support.

Eclética Química Journal, vol. 43, n. 4, 2018, 44-49
ISSN: 1678-4618
DOI: 10.26850/1678-4618eqj.v43.4.2018.p44-49

6. References

[1] von Hippel, P., Johnson, N., Marcus, A., 50 years of DNA 'Breathing': Reflections on Old and New Approaches, Biopolymers 99 (12) (2013) 923-954. https://doi.org/10.1002/bip.22347.

[2] Hidayat, W., Sulaiman, A., Viridi, S, Zen, F. P., The viscous and external forces effect on the thermal denaturation of Peyrard-Bishop, Physical Chemistry & Biophysics 5 (5) (2015) 1-5 (186). https://doi.org/10.4172/2161-0398.1000186.

[3] Flach, S., Gorbach, A., Discrete breathers-Advance in theory and applications, Physics Reports 467 (1-3) (2008) 1-116. https://doi.org/10.1016/j.physrep.2008.05.002.

[4] Mackay, R. S., Aubry, S., Proof of existence of breathers for time-reversible for Hamiltonian networks of weakly coupled oscillators, Nonlinearity 7 (1994) 1623-1643. https://doi.org/10.1088/0951-7715/7/6/006.

[5] Cuevas J., Localizacion y Transferencia de Energia en Redes Anarmónicas No Homogéneas, Ph. D. Thesis, Universidad de Sevilla, Sevilla, España (2003). http://grupo.us.es/gfnl/thesis.htm.

[6] Aubry, S., Cretegny, T., Mobility and Reactivity of Discrete Breathers, Physica D 119 (1-2) (1998) 34-46. https://doi.org/10.1016/S0167-2789(98)00062-1.

[7] Ambjomsson, T., Banik, S. K., Krichevsky, O., Metzler, R., Breathing dynamics in Heteropolymer DNA, Biophysics J. 92 (8) (2007) 2674-2684. https://doi.org/10.1529/biophysj.106.095935.

[8] Cortez, H., Drigo Filho, E., Ruggiero, J. R., Breather stability in one dimensional Lattices with a symmetric Morse Potential, TEMA, Tend. Mat. Apl. Comput. 9 (2) (2008) 205-212. https://doi.org/10.5540/tema.2008.09.02.0205.

[9] Cortez, H., Drigo Filho, E., Ruggiero., J. R., Cortez, M., Mobile breathers in a nonlinear model for DNA breathing, Eclética Química Journal 42 (2017) 71-75. https://doi.org/10.26850/1678-4618eqj.42.1.2017.p71-75.

[10] Sulaiman, A., Zen, F. P., Alatas, H., Handoko, L. T., Dynamics of DNA breathing in the Peyrard-Bishop weth damping and external force, Physica D 241 (2012) 1640-1647. https://doi.org/10.1016/j.physd.2012.06.011.

[11] Cortez, H., Tese de doutorado, Modelo Dinâmico e estatístico aplicado à transição de fase. UNESP.(2009) https://repositorio.unesp.br/bitstream/handle/11449/100461/cortezgutierrez_ho_dr_sjrp.pdf?sequence=1&isAllowed=y.

[12] Cortez, H., Drigo Filho, E., Ruggiero, J. R., Gutierrez, M. C., Fuentes Rivera, L. C., Thermodynamics of DNA with "hump" Morse potential, Eclética Química Journal 41 (2016) 60-65. https://doi.org/10.26850/1678-4618eqj.v41.1.2016.p60-65.

[13] Bustamante, C. Smith, S.B., Liphardt,J., Smith, D., Single-molecule studies of DNA mechanics, Current Opinion in Structural Biology 10 (3) (2000) 279-285. https://doi.org/10.1016/S0959-440X(00)00085-3.

Eclética Química Journal, vol. 43, n. 4, 2018, 44-49
ISSN: 1678-4618
DOI: 10.26850/1678-4618eqj.v43.4.2018.p44-49